ANL/NE-15/7

UV-Vis Spectroscopy as a Tool for Safeguards; Instrumentation Installation and Fundamental Data Collection

Project Final Report

Nuclear Engineering Division

About Argonne National Laboratory
Argonne is a U.S. Department of Energy laboratory managed by UChicago Argonne, LLC under contract DE-AC02-06CH11357. The Laboratory's main facility is outside Chicago, at 9700 South Cass Avenue, Argonne, Illinois 60439. For information about Argonne and its pioneering science and technology programs, see www.anl.gov.

DOCUMENT AVAILABILITY

Online Access: U.S. Department of Energy (DOE) reports produced after 1991 and a growing number of pre-1991 documents are available free via DOE's SciTech Connect (http://www.osti.gov/scitech/).

Reports not in digital format may be purchased by the public from the National Technical Information Service (NTIS):
U.S. Department of Commerce
National Technical Information Service
5301 Shawnee Road
Alexandria, VA 22312
www.ntis.gov
Phone: (800) 553-NTIS (6847) or (703) 605-6000
Fax: (703) 605-6900
Email: **orders@ntis.gov**

Reports not in digital format are available to DOE and DOE contractors from the Office of Scientific and Technical Information (OSTI):
U.S. Department of Energy
Office of Scientific and Technical Information
P.O. Box 62
Oak Ridge, TN 37831-0062
www.osti.gov
Phone: (865) 576-8401
Fax: (865) 576-5728
Email: **reports@osti.gov**

Disclaimer
This report was prepared as an account of work sponsored by an agency of the United States Government. Neither the United States Government nor any agency thereof, nor UChicago Argonne, LLC, nor any of their employees or officers, makes any warranty, express or implied, or assumes any legal liability or responsibility for the accuracy, completeness, or usefulness of any information, apparatus, product, or process disclosed, or represents that its use would not infringe privately owned rights. Reference herein to any specific commercial product, process, or service by trade name, trademark, manufacturer, or otherwise, does not necessarily constitute or imply its endorsement, recommendation, or favoring by the United States Government or any agency thereof. The views and opinions of document authors expressed herein do not necessarily state or reflect those of the United States Government or any agency thereof, Argonne National Laboratory, or UChicago Argonne, LLC.

ANL/NE-15/7

UV-Vis Spectroscopy as a Tool for Safeguards; Instrumentation Installation and Fundamental Data Collection

Project Final Report

by
Nicholas A. Smith, John F. Krebs, and Andrew S. Hebden
Nuclear Engineering Division, Argonne National Laboratory

September 20, 2015

EXECUTIVE SUMMARY

Two spectrophotometric process monitors, one optimized for high concentration (approximately 10 g/L) and one for trace levels (approximately 10 ppm), were developed at Argonne National Laboratory and installed at the Savannah River Site (SRS) H-Canyon facility for field testing. These systems were built of commercial off-the-shelf components utilizing a custom, facility-specific hardware interface. The systems directly provide a qualitative measurement of process chemistry (i.e., valence state). With appropriate calibrations, the systems could provide quantitative data. Laboratory tests were performed to determine the spectrophotometric molar absorptivity coefficients for relevant actinide and transition metals of interest.

CONTENTS

EXECUTIVE SUMMARY ..... **i**

1 INTRODUCTION **1**

2 SPECTROSCOPIC THEORY OF OPERATION **2**

3 HARDWARE DEVELOPMENT **4**

3.1 Spectroscopy System 4
3.2 Micro Flow Cell 4
3.3 Long Pathlength Flow Cell 5
3.4 Air/Gas Separation System 6

4 SOFTWARE DEVELOPMENT **8**

4.1 PUMAS 1.0 8
4.2 PUMAS 2.0 9

5 FIELD TESTS **10**

5.1 Micro Flow Cell 10
5.1.1 Normal Operation 10
5.1.2 Off-Normal Condition Detection 10
5.1.3 Transient Monitoring 11
5.2 LPFC 12

6 SPECTROSCOPIC DATA COLLECTION **16**

6.1 Plutonium (IV) 17
6.2 Uranyl ion 18
6.3 Chromium (VI) 20
6.4 Chromium (III) 21
6.5 Iron (III) 22
6.6 Nickel (II) 23

7 PROJECT SUMMARY **26**

8 REFERENCES **27**

APPENDIX A ANNOTATED BIBLIOGRAPHY **29**

APPENDIX B METHODOLOGY **39**

FIGURES

1 Micro flow cell. 5

2 A long path length flow cell. 5

3 CAD drawing of the micro flow cell and degassing system. 6

4 Detection of off-normal conditions. 11

5 PUMAS transient monitoring. 12

6 Spectra obtained from the LPFC. 13

7 Comparison of flowing, stagnant transmission of light through LPFC. 14

8 Plutonium (IV) spectral data. 17

9 Uranyl spectral data. 19

10 Chromium (VI) spectral data. 20

11 Chromium (III) spectral data. 21

12 Iron spectral data. 22

13 Nickel spectral data. 24

B-1 Double-beam spectrometers from the Agilent Cary line. 40

B-2 Example macro, semi-micro, and micro volume cuvettes. 41

TABLES

1 Summary of data collected for molar absorptivity measurements. 17

2 Molar absorptivity values (L mol^{-1} cm^{-1}) for Pu(IV) in 2–8 M HNO_3. 18

3 Molar absorptivity values (L mol^{-1} cm^{-1}) for UO22+ in 2–8 M HNO_3. 19

4 Molar absorptivity values (L mol^{-1} cm^{-1}) for Cr(VI) in 2–8 M HNO_3. 21

TABLES (CONT.)

5 Molar absorptivity values (L mol^{-1} cm^{-1}) for Cr(III) in 2–8 M HNO_3. 22

6 Molar absorptivity values (L mol^{-1} cm^{-1}) for Fe(III) in 2–8 M HNO_3. 23

7 Molar absorptivity values (L mol^{-1} cm^{-1}) for Ni(II) in 2–8 M HNO_3. 24

1 INTRODUCTION

This project was a multi-year effort to develop commercial off-the-shelf (COTS) spectroscopic components into an in-line, near-real-time accountancy instrument, and field test this instrument. This type of monitor is important for a variety of reasons. With appropriate calibrations, real-time information can be obtained on process chemistry or on the amount of material moving through a process or present in a tank. This information can be vital to understanding the nature of processes (normal vs. upsets/off-normal conditions), as well as improving estimates of the amount of material involved in specific processes. These estimates can then be used to increase the time between accountancy periods or reduce the required manpower commitment for international inspections, which in turn would increase the operational envelope of safeguarded facilities.

Because this system is designed to make point measurements, it was envisioned that multiple systems would be deployed when monitoring a complex process. Therefore, a modular construction methodology using COTS components was a high priority. By emphasizing COTS and reducing the number of custom parts that would need to be fabricated, the costs of installation and maintenance would be minimized. This strategy would also allow components to be replaced on an as-needed basis (rather than replacing the entire system), which will reduce the lifetime costs of the system.

Two complete systems were installed and tested at the Savannah River Site (SRS) H-Canyon facility as part of the National Nuclear Security Administration (NNSA) Safeguards Test Bed program. This field test experience provided valuable feedback for the system design so that it could be adapted for use in an operational environment. In addition, the spectrophotometers were valuable to the H-Canyon operations staff because they allowed real-time measurement of the valence state of tank materials. This field test provided a logical conclusion to the project by demonstrating the functionality of the system, as well as the value provided to the customer.

2 SPECTROSCOPIC THEORY OF OPERATION

Absorption spectrophotometers operate by measuring the change in light transmitted through a sample. This relationship is governed by the Beer-Lambert Law, shown in Equation 1. As the concentration, c, of a molecule increases, measured through a given path length, l, it absorbs more light at characteristic wavelengths and decreases the transmission of light through the sample. The transmittance (T) is measured and converted to absorbance (A) by taking the negative logarithm of the transmittance. The molar absorptivity, ε, is the constant of proportionality for this equation, is dependent on the solution conditions (ionic strength, ligands, speciation, etc.), and must be experimentally determined. Because each molecule can absorb light at multiple wavelengths, multiple species can absorb light at the same wavelength. In these cases, the observed absorbance is equivalent to the sum of the individual absorbances.

$$A = -\log(T) = \varepsilon \cdot c \cdot l \qquad \text{Equation 1}$$

In practice, the transmittance is measured by analyzing the light source intensity in the absence of the analyte, referred to as the reference intensity, I_{Ref}, and in the presence of the analyte, referred to as the sample intensity, I_{Sam}. The reference intensity could be an empty sample holder, a sample holder filled with the matrix solution (e.g., water, acid), or air. These two quantities are divided ($I_{\text{Sam}}/I_{\text{Ref}}$) to produce the transmittance and, subsequently, the absorbance.

This relationship is further altered by the introduction of a detector dark current. As a general rule, most photon-sensitive detectors will have some characteristic background signal. For absorption spectrophotometers, this can be interpreted as a phantom current generated in either the solid state detector or on the voltage readout of the photomultiplier tube in larger system. This dark current is assumed to be constant over short timescales. The intensity measurements, which are simply binned counts collected over a specified collection (integration) time on the detector, must be corrected for this dark current prior to calculating a transmittance Equation 2:

$$T = \frac{(I_{Sam} - I_{Dark})}{(I_{Ref} - I_{Dark})} \qquad \text{Equation 2}$$

Commercially available spectrometers and light sources generally operate in one of two modes: single or double beam. In single beam mode, one light path is used to measure I_{Sam} and I_{Ref}, generally in sequence. A static I_{Ref} is valid as long no changes are made to the system and the detector response and light source output remain constant. This assumption is only valid over short time periods, requiring frequent re-collection of I_{Ref}. In a double beam spectrometer, the I_{Sam} and I_{Ref} are collected at every point throughout the measurement using two beam paths; one beam path holds the sample, the other path holds a reference sample (as above, an empty cell, matrix blank, or air). Internal optics and temporal resolution allow measurement of I_{Ref} and I_{Sam} at every measurement point using the same light source within very short timescales. This ensures that the light source and detector responses should be essentially identical. A double beam system generally needs an additional measurement, a blank. The system needs to measure

the relative difference in transmission between the two beam paths, which is not guaranteed to be identical. This is done by measuring a blank in the sample position, generally using the same composition as the reference position, which allows the spectrometer to determine where the relative "zero" of the system is.

Neither of these systems would be suitable for installation in an operational facility such as H-Canyon. There was not a practical way to re-collect reference solutions during extended operation (indicating a water flush of the cell), as would be required for single-beam systems. Similarly, the engineering that would be required to fabricate a true, remote, double-beam spectrometer would be beyond the scope of this project. Therefore, the system employed what we are terming a "pseudo-double beam" system. In this configuration, the system operates two cells, a sample cell and a reference cell, to collect the I_{Sam} and I_{Ref}, similar to a double-beam system. However, the reference position is only collected at specified intervals, similar to a single-beam system. At the start of operations (and at extended intervals afterwards, such as a day or week) a system blank must be recorded in the sample position, equivalent to the double-beam blank. This allows the system to determine the true system zero, with respect to a static reference cell, and then continually correct the sample absorbance for variations in the light source and detector. As an additional check, a second pair of channels are setup to measure an absorbance standard (holmium or neodymium glass paired with a quartz blanks) to provide a both a wavelength calibration and system check. An important caveat to this system is that the reference solution does not have to match the process cell with respect to size, location, or integration time, as long as a blank in the process cell is collected.

3 HARDWARE DEVELOPMENT

The hardware development phase of this project was pursued on multiple fronts: integration of the spectroscopic system, evaluation of flow cells, and the development of a passive air/gas separation system. These tasks were iteratively pursued throughout the first 2 years of the project leading up to installation at H-Canyon. In addition to sourcing COTS components that would survive the harsh environment in a reprocessing plant (nitric acid, reactive metals, radiation, etc.), all materials had to meet the stringent safety codes required at the H-Canyon facility.

3.1 SPECTROSCOPY SYSTEM

Two spectroscopy systems were assembled from COTS components for deployments in Fiscal Year 2013 (FY13) and Fiscal Year 2014 (FY14). The first spectroscopic system, used with the micro flow cell (below) used an AvaSpec-2048-USB2-UA spectrometer and an AvaLight-DH-S-BAL light source, both from Avantes, Inc., and are currently installed at H-Canyon. In addition, two Agiltron LightBend 1×4 broadband fiber optic bidirectional switches that operate in the 200–2000 nm wavelength range are installed to switch between channels. Due to legal interferences, the FY14 system developed for the Long Pathlength Flow Cell (below) uses a 2×8 port Avantes Fiber Optic Multiplexer. In both configurations, the switch(es) is (are) connected via optical fibers to the sample cell in the H-Canyon sample aisle; a reference cell, either in the sample aisle or in the control room; and two cuvette holders in the control room that house a holmium wavelength standard and its reference.

Based on performance of the systems, the Agiltron switches would be preferred over the Avantes multiplexer (if supply chain issues are resolved). There is a smaller discontinuity after cycling between inputs, which improves collection statistics, and the units are significantly less expensive.

3.2 MICRO FLOW CELL

In order to measure very concentrated solutions with a high absorbance, one must either increase detector sensitivity to allow high (>2) absorbance numbers or reduce the pathlength of the measurement, per Equation 1. A set of reduced pathlength flow cells were purchased from Custom Sensors & Technology (CST), Inc. (see Figure 1). These cells use two optical interface couplers (OICs) with sapphire windows and Chemraz seals, to couple a pair (in/out) of fiber optic cables. The OICs could be positioned in the housing with separations ranging from 0.1 to 10 mm. The flow path was equipped with standard 0.25-inch compression fittings.

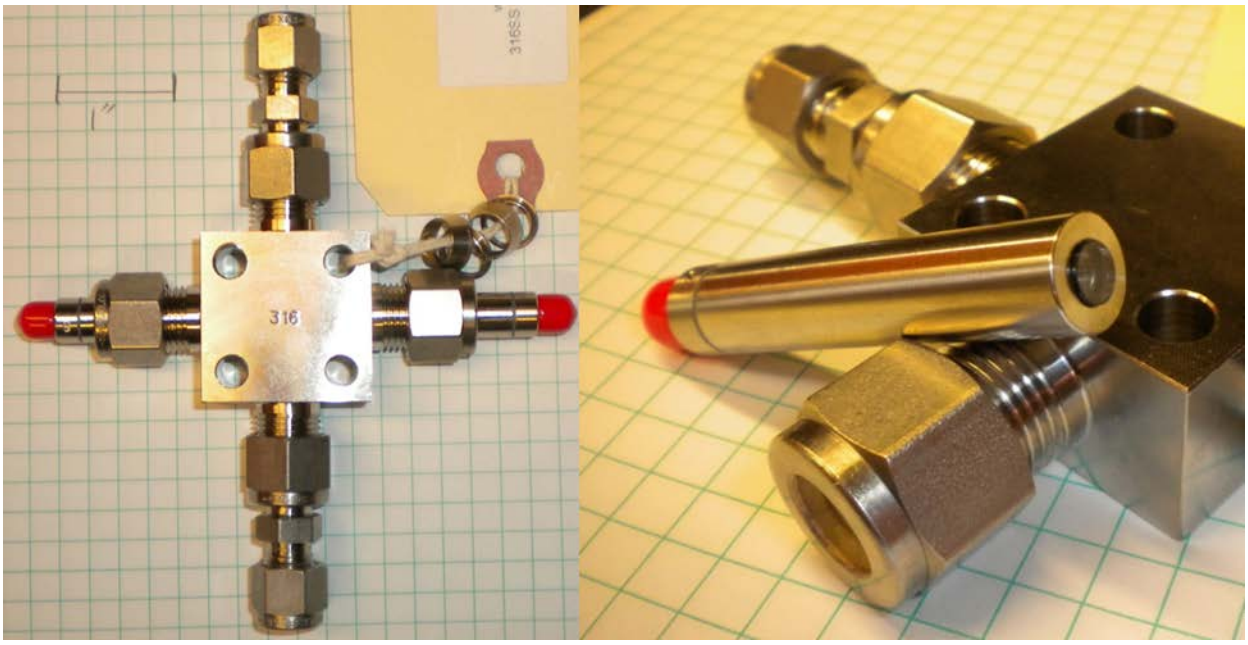

Figure 1—Micro flow cell. Left: assembled with the solution flow path oriented vertically and the light path horizontal. Right: with the optical interface coupler removed showing the sapphire window.

3.3 LONG PATHLENGTH FLOW CELL

For low-concentration streams, a second flow cell was purchased from Custom Sensor Technologies (via Ocean Optics) with a pathlength of 50 cm; this is referred to as a Long Pathlength Flow Cell (LPFC). Again, sapphire windows and Chemraz seals were employed on the OICs. A short version (10 cm) is shown in Figure 2.

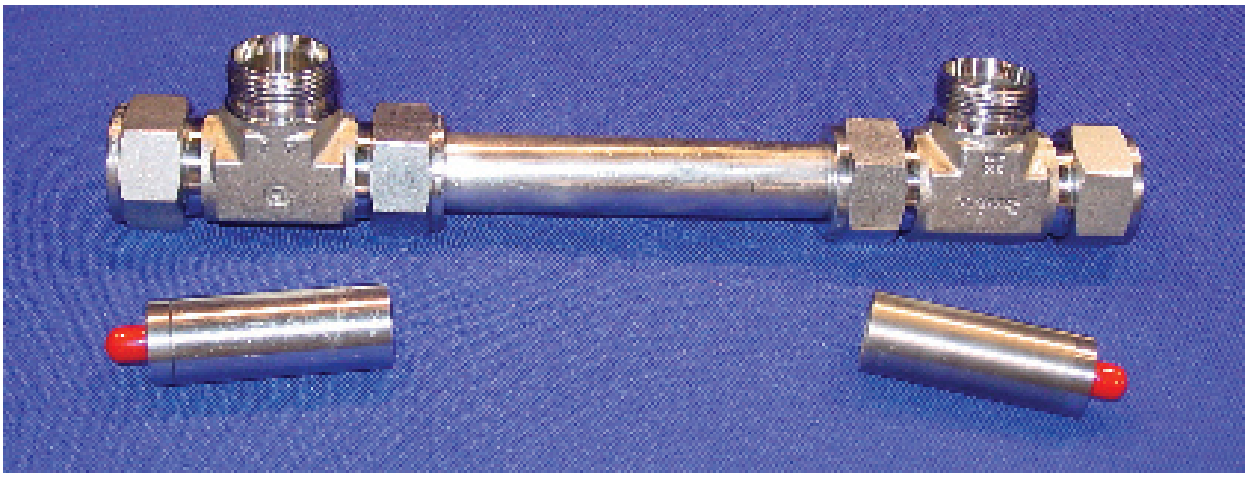

Figure 2 – A long pathlength flow cell. This unit is approximately 10 cm long, shown with the optical interface couplers removed. Flow cell provided by Custom Sensors and Technology, Fenton, MO (covered under US Patent #5,408,313).

3.4 AIR/GAS SEPARATION SYSTEM

While COTS solutions are preferred, each operational facility will have slightly different equipment to be interfaced to the spectrometer. Therefore a custom interface needed to be fabricated. The process samples at H-Canyon could contain up to 90% entrained air due to the pneumatic sample transport system. The hardware would be installed within a sample collection and designed to not impact the operation of the sampler. Argonne and SRS staffs consulted to design and fabricate a custom component to remove the entrained air from the process solution. Referred to as a degasser, this component separated the liquid and gas phases of the process stream. The liquid phase was routed through the flow cell while the gas component bypassed the cell entirely. Downstream of the flow cell and the grab sample port, the gas and liquid streams were joined prior to being returned to process stream. The engineering drawings featuring the micro flow cell and degasser are shown in Figure 3.

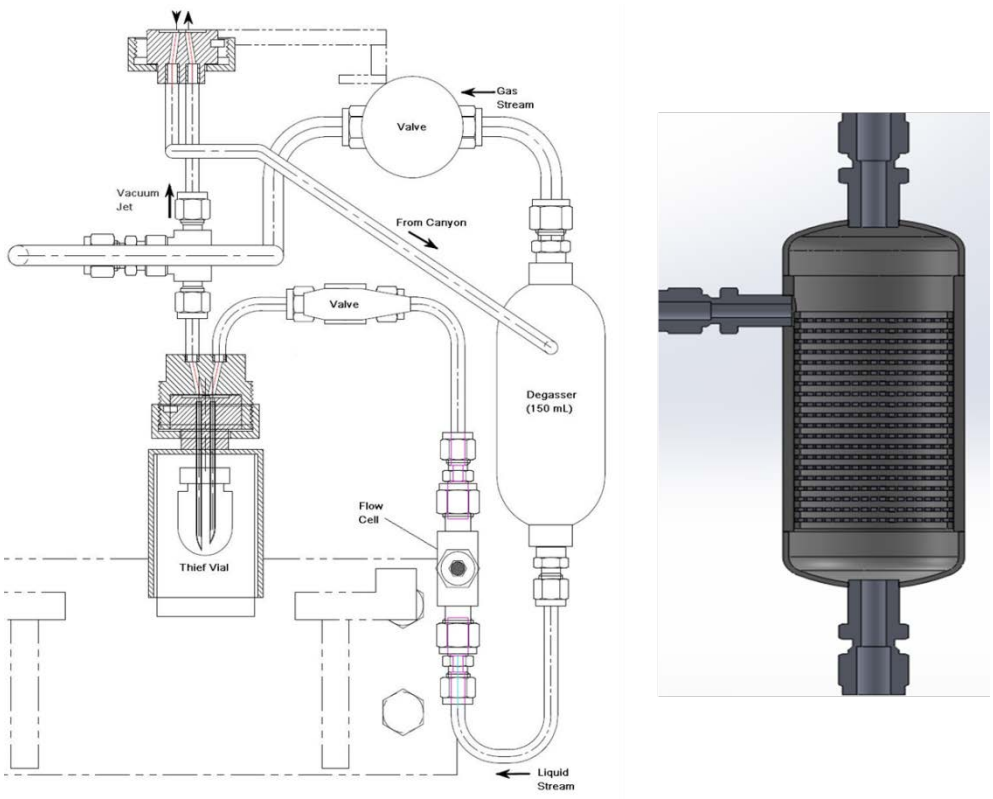

Figure 3—CAD drawing of the micro flow cell and degassing system. The configuration on the left represents the system as installed with the micro flow cell suitable for integration into the H-Canyon sampler box. The improved degasser with internal mesh structures is shown on the right.

A similar unit was prepared for the LPFC with the addition of a custom Lexan box housing fabricated by SRS. An improved degasser was also developed for this installation that incorporated internal mesh structures to enhance the coalescence of entrained gas bubbles. This was further refined by using a finer thread valve on the gas stream to control the flow through the degasser.

4 SOFTWARE DEVELOPMENT

In order to integrate the various hardware components and collect meaningful data, a custom control software package needed to be developed. The LabVIEW runtime environment was chosen due to the existence of existing control packages for the Avantes hardware, as well as previous Argonne experience using the software. This control package was loaded behind a graphical user interface that allowed full control of the various hardware components. In addition to data-logging capabilities, real-time graphical displays were added for immediate data review and analysis. The system was dubbed the Plutonium-Uranium Monitoring and Acquisition Software, or PUMAS.

4.1 PUMAS 1.0

An operating version of PUMAS was initially completed in the third quarter of Fiscal Year 2012 (FY12). Features of that version included recording absorbance and raw intensity (i.e., scope mode) spectra and the ability to monitor absorbance for user-selectable wavelengths. The single wavelength absorbances are plotted in chart mode affording a time-dependent visual representation to aid the operator in real-time process monitoring. The capability to monitor the absorbance values at additional single wavelengths was implemented in the fourth quarter of FY12. Currently, the single wavelength absorbance is plotted in chart mode affording a time-dependent visual representation of the values as they are collected.

PUMAS runs in the National Instruments LabVIEW environment, and uses the AS-5216 Dynamic Link Library (DLL) provided by Avantes, Inc., to control the AvaSpec-2048-USB2-UA spectrometer and the AvaLight-DH-S-BAL light source. In the system configuration installed with the micro flow cell at H-Canyon, PUMAS controls two Agiltron LightBend 1×4 Broadband Fiber Optic bidirectional switches that operate in the 200–2000 nm wavelength range. The switches are connected via optical fibers to the sample and reference cells in the H-Canyon sample aisle, and to two cuvette holders in the control room that house a holmium wavelength standard and its reference.

Currently, PUMAS collects data to calculate both a calibration absorbance spectrum and a process sample absorbance spectrum. Once calculated, each absorbance spectrum then undergoes a baseline adjustment, using the water blank spectrum, and individual absorbance values are then read from the baseline-corrected absorbance spectrum. PUMAS then charts the absorbance values of selected wavelengths of interest for both the process sample and the calibration standard over time. For the process sample, the absorbance values are converted to concentrations and plotted. The variation in absorbance values are calculated using a pooled variance technique. PUMAS provides a comment box so that a log of observations made by the operators can be created. Comments are timestamped so that they can be cross-referenced to the timestamps in the recorded data files. The frequency of the calibration checks, the number of scans performed, and the spectroscopic parameters (the number of averaged scans and the detector integration time) are user-adjustable parameters.

4.2 PUMAS 2.0

The first version of PUMAS required that the integration times for both the sample and reference cell be identical. This led to a situation where an integration time short enough to prevent saturation of the detector in the reference channel was barely sufficient to collect a signal in the sample channel. This situation would be exacerbated with the deployment of the LPFC. After examination of the underlying principles behind the pseudo-double beam system—assuming a blank was collected the integration times for the sample and sample reference channels no longer needed to be linked—this required a redesign of the software to incorporate the new design requirement.

For the LPFC, the two Agiltron switches were replaced by a single Avantes Fiber Optic Multiplexer (FOM). The FOM unit (FOM-UVIR400-2x8) directs one pair of input/output channels through eight paths. Although eight paths are possible, only four paths (sample, sample reference, wavelength calibration standard, and wavelength calibration standard reference) were required for LPFC operation. The PUMAS 2.0 software includes functionality to select which type of fiber optic multiplexer is being used. The PUMAS 2.0 software was successfully tested in mid-fourth-quarter FY15 with the previously installed micro flow cell equipment to verify operability with the Agiltron switches.

5 FIELD TESTS

Both the flow cells were sent to the SRS H-Canyon facility for installation and testing under operational conditions. This required a significant amount of coordination between the Argonne and SRS staff to ensure that the cells would be operational and acceptable. The in-line micro flow cell, installed in March 2013, performed well and was instrumental in detecting an off-normal oxidation state in the tank with subsequent validation with Savannah River National Laboratory (SRNL) analytical results. The real-time identification of this off-normal condition allowed SRS operations to plan and execute a chemical treatment corrective action prior to sending the tank contents to the next unit operation. The micro flow cell proved valuable enough that in mid-2015, this temporary modification of the plant became a permanent modification of the SRS H-Canyon operations. The LPFC that was to be installed at the end of FY14 was successfully installed and tested in mid-fourth-quarter FY15.

5.1 MICRO FLOW CELL

5.1.1 Normal Operation

The associated hardware for the micro flow cell (see Figure 3) was fabricated and installed by SRS H-Canyon staff in the sampling aisle. Once the hardware was in place in the sampler housing, the final spectroscopic hardware was installed and tested by SRS and Argonne staff. Once installed and adjusted, it was possible to successfully log multiple hours of spectroscopic data.

Due to an unexpected oxidation state shift (see below), as well as higher than expected concentrations of transition metals, a full quantitative analysis using PUMAS could not be completed. However, several qualitative modes of operation were successfully demonstrated that extend the application of this technology beyond concentration measurements. The system allows the operator/inspector to track specific absorbance bands over time to verify stable process operation, detect off-normal conditions, monitor a planned change in chemistry, or detect an unscheduled change.

5.1.2 Off-Normal Condition Detection

During the initial setup and testing of the micro flow cell system, spectra were recorded and evaluated by Argonne and SRS personnel in real time. It was observed that the spectrum had deviated from the expected conditions and indicated that the solution chemistry had shifted. Specifically, the solutions showed clear indications of Pu(VI) in a solution that should have been exclusively Pu(IV). This shift was apparent in the presence of an oxidized species, PuO_2^{2+}, in the spectrum, shown in Figure 4. This signal, acquired in real time, was used to justify an additional analysis of the process solution to verify the oxidation state of the tank solution. Detection of an off-normal condition is an important tool for both operations and inspections personnel because

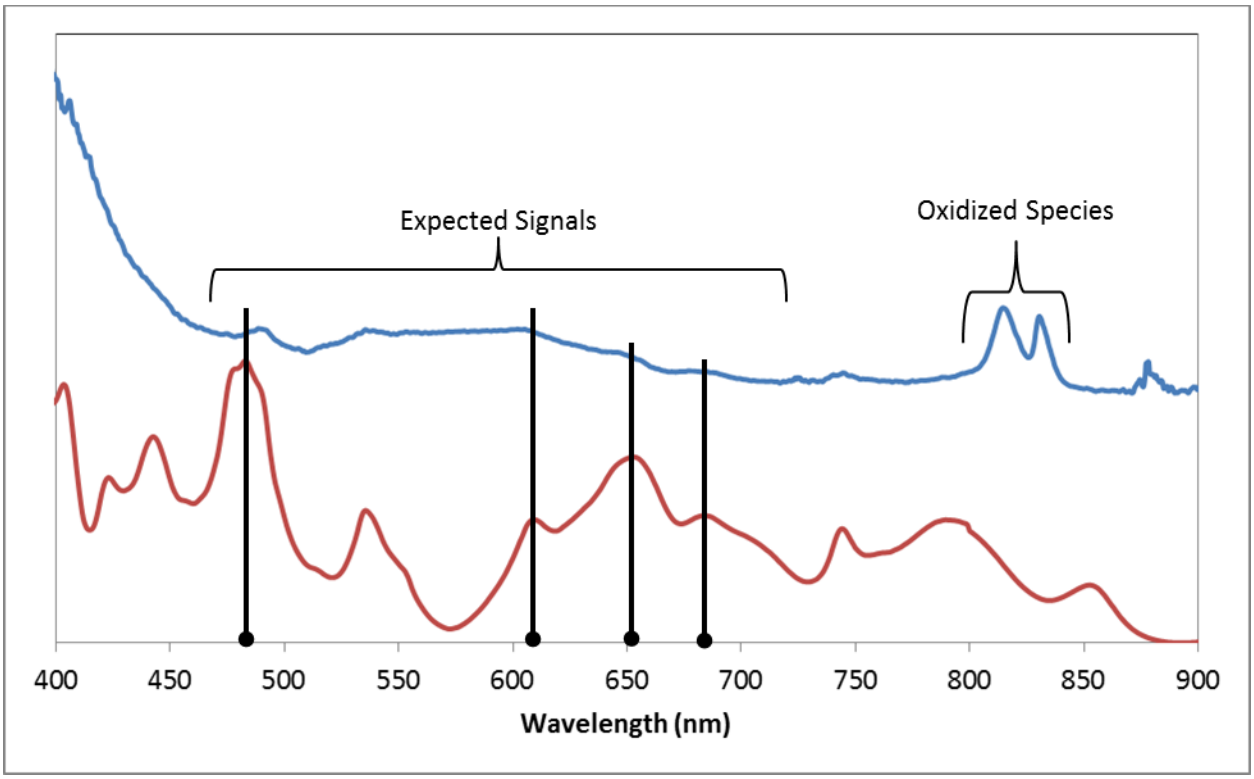

Figure 4—Detection of off-normal conditions. A comparison of the process spectrum (blue, upper line) to the expected spectrum (red, lower line) revealed that the process stream contained $Pu^{4+/6+}$; analytical results also showed a number of corrosion products (chromium, iron, etc.). The process solution was expected to contain only Pu(IV).

off-normal conditions can indicate that a process upset or diversion attempt has been made and that additional actions or confirmations are required.

5.1.3 Transient Monitoring

The correction of the oxidation state imbalance shown in the previous example was also monitored with the micro flow cell system. By adding a reducing agent to the process stream, a planned transient was introduced into the system; this could be monitored similarly to an unplanned transient as well. The data in Figure 5 was collected in real time without additional processing (save for presenting the time dependent data as a waterfall plot). Starting about midway through the plot, the data clearly shows a change in the absorption spectrum, which indicates a reduction of the PuO_2^{2+} to Pu^{4+}. The fast response of the system enabled this type of real-time monitoring. The change in concentration and speciation was also evident in the strip chart readout, which clearly showed wavelengths corresponding to the oxidized plutonium decreasing concurrently with increases in the wavelengths associated with tetravalent plutonium.

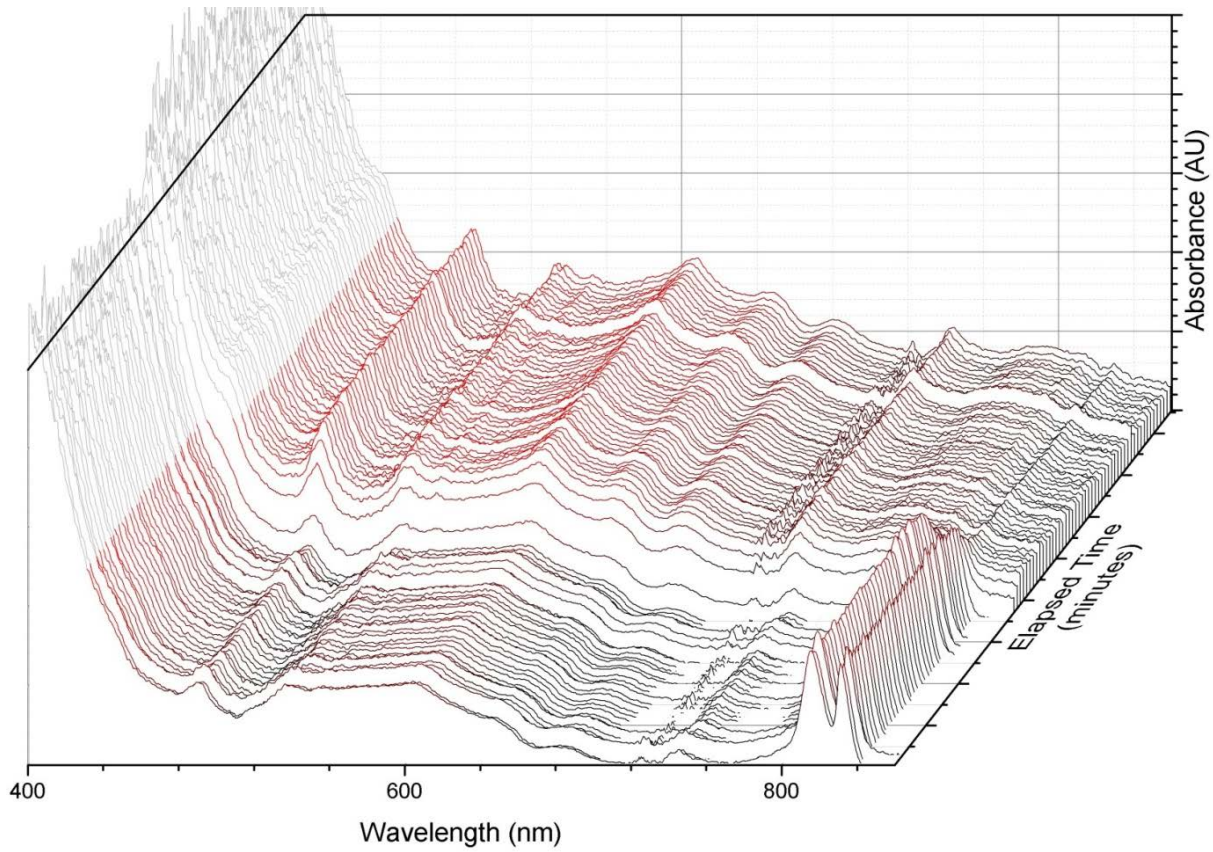

Figure 5—PUMAS transient monitoring. Waterfall plot of PUMAS data during a transient operation (elapsed time increases from the foreground to the background). The change to the process stream chemistry is evident approximately halfway through the plot, where the sharp peaks above 800 nm are reduced and the peaks between 440 and 660 nm are enhanced.

5.2 LPFC

The installation of the LPFC was completed in the fourth quarter of FY15 by SRS and Argonne staff. The system was found to have improved solution flow through the cell, as evidenced by the lack of bubbles in the system (which have a distinct spectroscopic signal) and a faster establishment of steady flow. This is likely due to one of two factors (or a combination of both): the incorporation of a valve with a finer control, or the improved degassing unit (Section 3.4).

When operating with a flowing tank solution, the unit produced signals with very low light transmittance, and thus a very high absorbance. This result was expected from bench-scale tests, though the magnitude of the issue was not. Conversations with SRS/SRNL staff led to the hypothesis that the viscosity of the tank solution combined with the flow pattern and flow rate were producing an optically opaque solution. This solution would scatter light due to solution lensing effects, which would result in a high absorbance. The proposed solution was to halt flow through the system and isolate a sample in the LPFC. This resulted in a stagnant sample that was “trapped” in the cell.

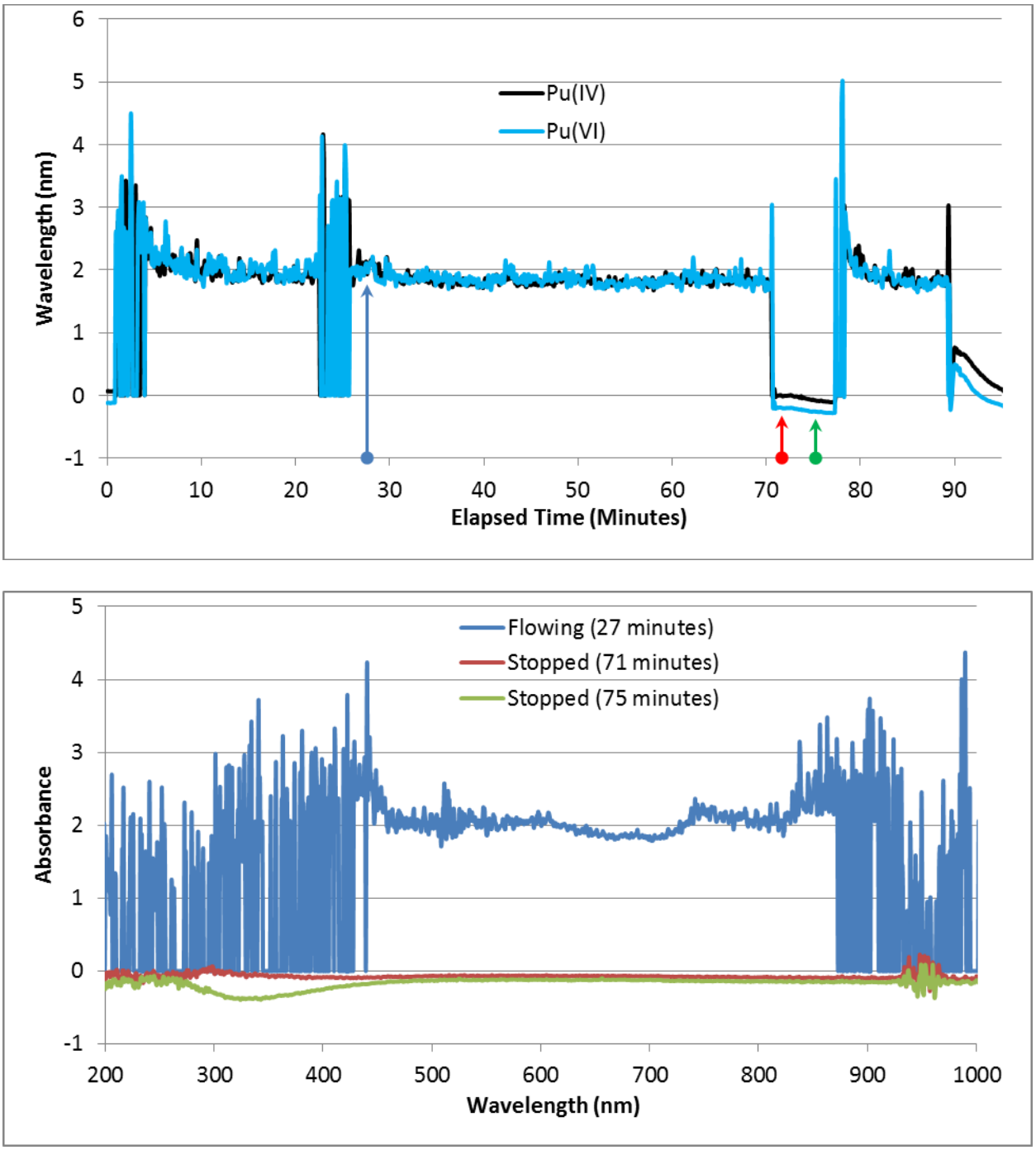

Figure 6—Spectra obtained from the LPFC. Top: two wavelengths monitored as a function of time. The disruptions at 0–5 minutes and 22–25 minutes are caused by altering the valve configuration and passing air through the cell (bubbles). At ~70 and 90 minutes, the system was successfully put into a mode that statically held a sample of the tank solution in the flow cell. Bottom: spectrum of the cell at three time points (denoted by colored arrows in the upper graph). When flowing, a large absorption is registered (blue); once the tank sample is static, the spectrum (red, green) drops back to the absorbance levels expected for a dilute solution.

The observed absorbance fell off immediately and the spectra that were collected were very similar to the water blank and more consistent with bench-scale test results.

Due to these results, it is the Argonne team's belief that high-fidelity data cannot be observed directly while the system is flowing. This is due to the very low amount of signal that is being transmitted, as shown in Figure 7. With signal transmission rates this low, a 20% reduction in light (corresponding to 0.1 absorbance units) would be virtually indistinguishable from noise. By stopping the solution inside the cell, the amount of light transmitted increases by 1–2 orders of magnitude, making measurements of small changes in absorbance possible.

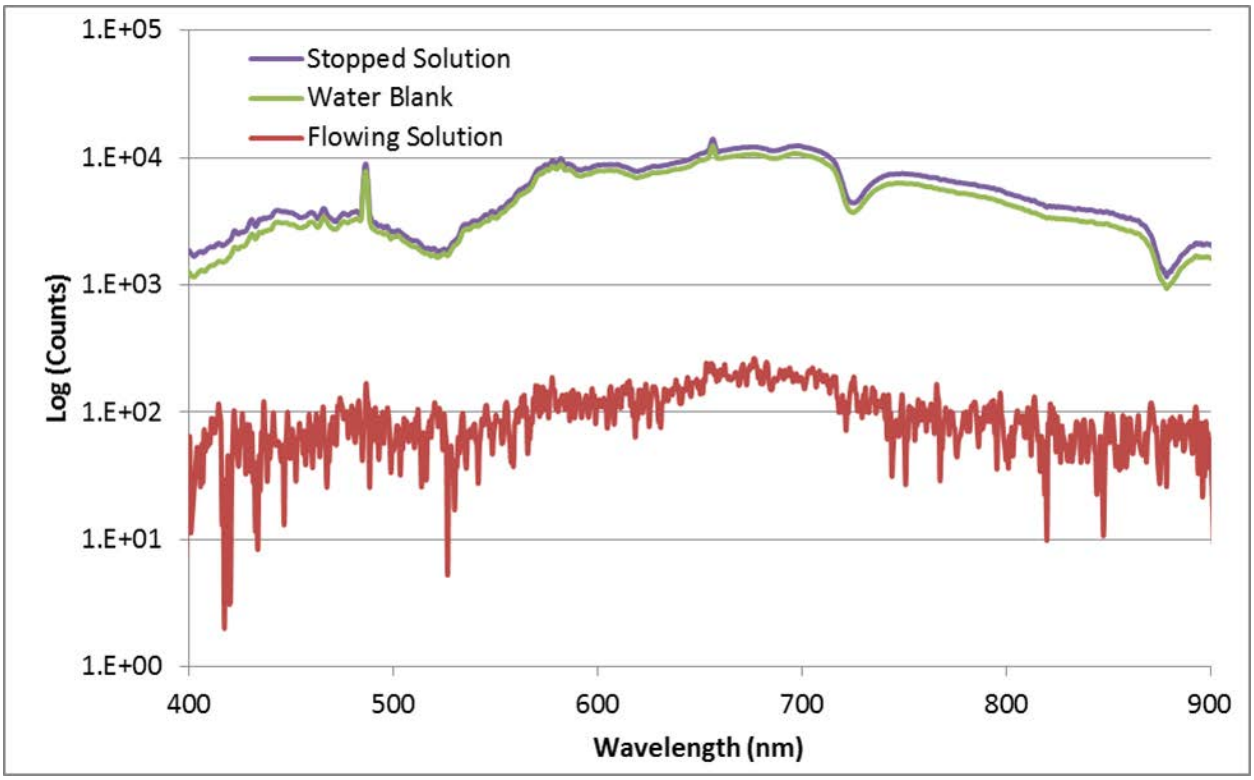

Figure 7—Comparison of flowing, stagnant transmission of light through LPFC. The red line shows the very low signal strength through the LPFC when the solution is flowing. Because of this, it is unlikely that a signal attributable to a particular chemical species could be detected in a flowing mode. Note: spectra were shifted upward by 100 counts to facilitate logarithmic plotting.

However, it remains to be seen whether the system can detect changes in specific wavelengths while flowing; there was not enough spectroscopically active material in the process tank to observe any chemical species in either mode. The estimated limits of detection—where a detectable signal is 0.1 absorbance units—for this system is 10–15 ppm for Pu(IV) at 480 nm , 10–15 ppm Pu(VI) at 814 nm, and 40–50 ppm for U(VI) at 420 nm. Additional spectroscopic and analytical results will need to be collected by the SRS staff as additions are made to the associated tank

Based on preliminary conversations with SRS/SRNL staff, there should have been enough material in the tank solution to produce an absorbance signal. The lack of this signal has not been adequately examined. However, it has been hypothesized that the metal species in the solution (determined via destructive analysis) may not have been solubilized but instead existed as a finely divided solid. In this case, the particles would not behave as a traditional solution but would instead diffuse the light from the light source. Depending on the size of the particles, the light can be diffracted, refracted, reflected or absorbed. It is highly unlikely that any light would be transmitted through the particle. Therefore, a true absorbance signal would not be obtained but instead a sloped spectrum would be obtained with higher absorbances at shorter wavelengths (Thomas, 2007, p. 152). This hypothesis would appear to be in conflict with an SRNL report that indicates that the majority of the metal should be solubilized (Nash, 2012). Furthermore, due to the particular chemistry present during this install (presence of oxalate), which is not indicative of future operations, this issue may not be present during future campaigns and a completely solubilize solution will be present. Therefore, it is imperative that additional data collections be made as the chemistry in the tank is changed.

6 SPECTROSCOPIC DATA COLLECTION

Experiences with the micro flow cell led to the conclusion that high-quality spectroscopic data needed to be collected under process conditions relevant to the canyon chemistry. The impact of dissolution products in the sample solution were an identified concern. Ideally, an advanced mathematical model (such as a principle component analysis) could be developed if suitable input datasets were available. A review of the relevant spectroscopic literature was developed during FY12 that demonstrated this fundamental knowledge gap (see Appendix A).

One of the main issues was that the existing literature generally failed to provide molar absorptivity coefficients with any associated errors, thus preventing inter-comparisons of the datasets. This was compounded by a lack of data at the higher nitric acid concentrations generally found under reprocessing conditions. Therefore, a methodology was developed to facilitate the measurement of molar absorptivity coefficients with an emphasis on tracking associated uncertainties. Compounding this problem is the fact that there is a measurable error in all of the quantities used to calculate the molar absorptivity constants (path length, absorbance, concentration. This problem, generally referred to as the “error in variables” problem, is resistant to standard regression techniques. Therefore, a new analysis method, utilizing a maximum likelihood estimation regime, was developed in conjunction with the Mathematics and Computer Science division at Argonne (see Appendix B).

Spectroscopic datasets were collected for tetravalent plutonium and the uranyl ion, as well as for the common stainless steel corrosion products of chromium, iron and nickel (Smith, 2015). These datasets were collected in varying concentrations of nitric acid. The transition metal concentrations were verified by inductively coupled plasma mass spectrometry (ICP-MS), the plutonium by radiometric analysis, and the uranium by direct gravimetric production.

Each curve in Figures 8–13 is generated by evaluating the molar absorptivity coefficient at several wavelengths under a constant matrix and decreasing metal concentrations. Each curve in the figures is a distinct experiment and not an average. Therefore, the table values, which are averages of multiple experiments, may not exactly match the figures. The wavelengths were chosen as the absorption at spectral peaks (if any were present) or as a uniform range in the case of more continuum-type absorbances. These coefficients are then used to generate a molar absorptivity curve through least squares regression between the coefficients and an exemplar spectrum (generally the highest concentration sample under similar conditions). A single replicate was run for each matrix composition for actinide species due to material usage constraints. The transition metal experiments were generally performed in duplicate, with the exception of trivalent chromium, which was analyzed in triplicate. The values reported in Tables 2–7 are the average coefficients and their associated errors (summed in quadrature from the regression analysis).

Table 1—Summary of data collected for molar absorptivity measurements.

Experimental parameters	Plutonium (IV)	Uranyl Ion	Chromium (VI)	Chromium (III)	Iron (III)	Nickel (II)
Acid concentrations investigated	2–8	2–8	1–8	1–8	1–8	1–8
Number of datasets per acid concentration	1	1	2	3	2	2
Number of samples (dilutions) per dataset	8	8	6	6	6	6

6.1 PLUTONIUM (IV)

Each plutonium solution was prepared fresh and analyzed immediately to minimize disproportionation at lower acid concentrations. The plutonium dataset shows a marked change in structure throughout the series, which is consistent with previous studies (Lee, 2007; Wilson, 2005). Although this study only examined nitric acid concentrations through 8 molar, it is recognized that an additional peak at 491 nm will appear at higher acid concentrations (Smith, 2010). This is an important note for process chemistries that may operate at extremely high acid concentrations.

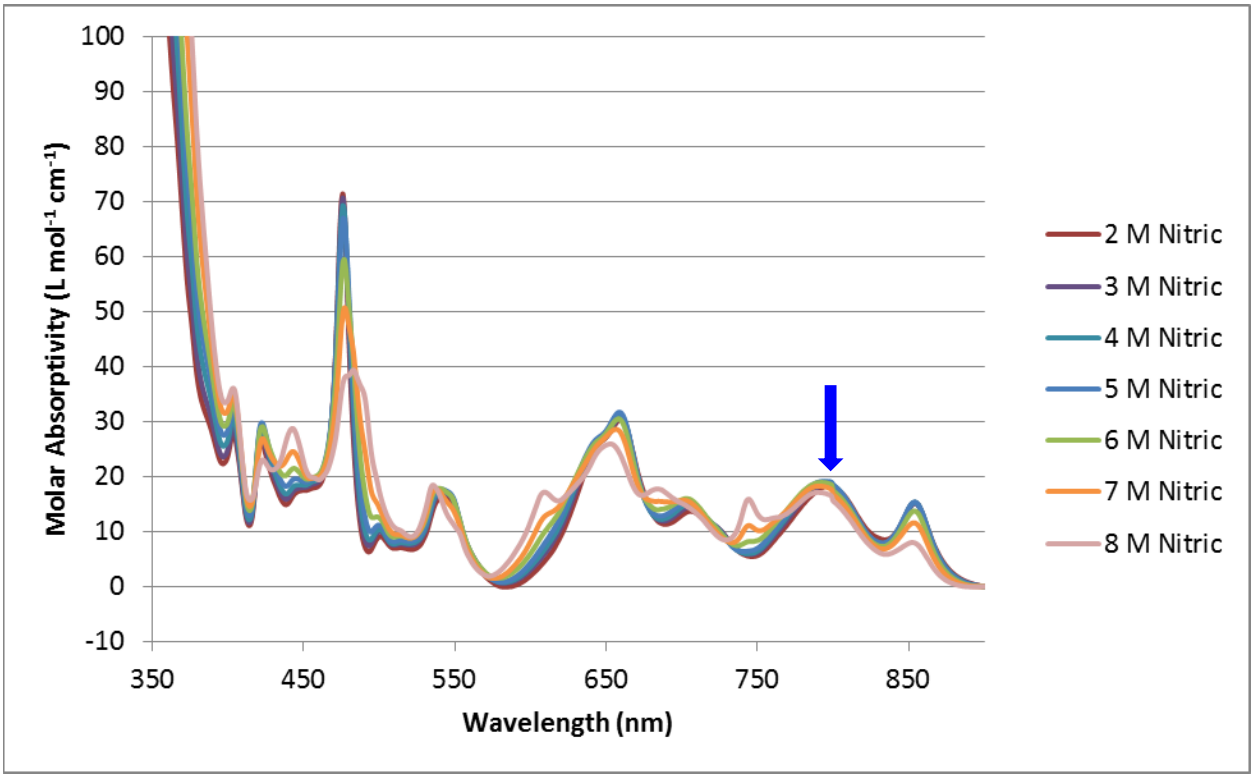

Figure 8—Plutonium (IV) spectral data. Data were collected in 1-cm poly(methyl methacrylate) (PMMA) cuvettes with increasing concentrations of nitric acid. A discontinuity in the data can be observed at ~800 nm (blue arrow), where the spectrometer source changeover occurs.

Table 2—Molar absorptivity values (L mol^{-1} cm^{-1}) for Pu(IV) in 2–8 M HNO_3.

Wavelength (nm)	Nominal nitric acid concentration (molarity)						
	2	3	4	5	6	7	8
404	27.9 ± 1.1	29.1 ± 1.1	30.4 ± 1.1	32.3 ± 1.2	33 ± 1.2	34.5 ± 1.3	36 ± 1.4
422	26.31 ± 0.99	27.9 ± 1.0	28.8 ± 1.1	29.7 ± 1.1	28.6 ± 1.1	26.55 ± 0.99	22.82 ± 0.86
443							28.6 ± 1.1
476	72.2 ± 2.7	70.7 ± 2.6	70.0 ± 2.6	67.1 ± 2.5	59.5 ± 2.2	50.0 ± 1.9	
483							39.2 ± 1.5
537							18.17 ± 0.69
543	11.35 ± 0.43	12.33 ± 0.46	11.99 ± 0.45	12.57 ± 0.47	12.28 ± 0.46	17.53 ± 0.65	
609							17.25 ± 0.65
653							25.92 ± 0.98
660	30.3 ± 1.1	30.6 ± 1.1	31.1 ± 1.2	31.4 ± 1.2	30.2 ± 1.1	27.8 ± 1	
684							17.86 ± 0.67
706	13.39 ± 0.51	14.58 ± 0.54	14.83 ± 0.55	15.49 ± 0.58	15.74 ± 0.59	15.28 ± 0.57	

6.2 URANYL ION

The spectra collected for the uranyl ion is similar to that found in the literature (Klygin, 1970; Lascola, 2002; Smith, 2010). The molar absorptivity coefficients are generally consistent, though slightly lower than Lascola, especially at higher nitrate concentrations.

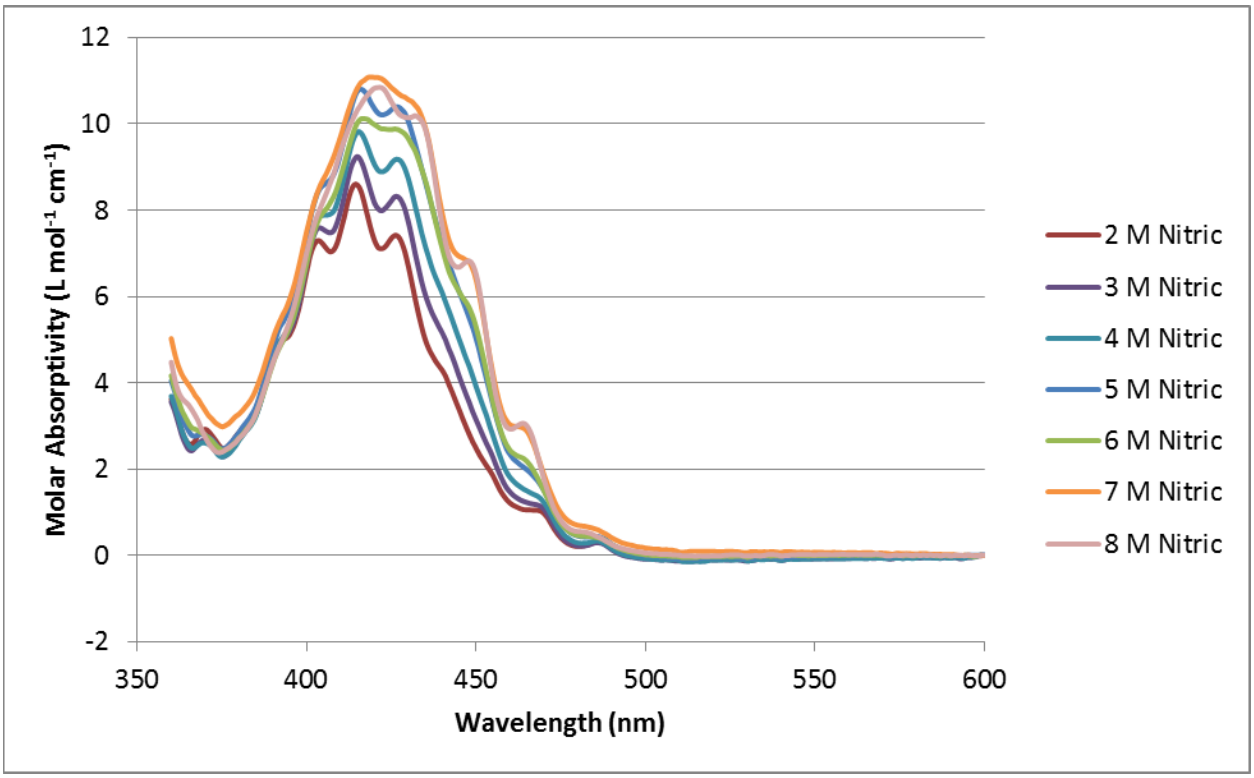

Figure 9—Uranyl spectral data. Data were collected in 1-cm PMMA cuvettes in increasing concentrations of nitric acid.

Table 3—Molar absorptivity values (L mol^{-1} cm^{-1}) for UO_2^{2+} in 2–8 M HNO_3.

Wavelength (nm)	Nominal nitric acid concentration (molarity)						
	2	3	4	5	6	7	8
392	4.9 ± 0.13	4.88 ± 0.13	4.82 ± 0.13	5.16 ± 0.14	4.79 ± 0.13	5.59 ± 0.15	4.96 ± 0.13
403	7.18 ± 0.19	7.42 ± 0.19	7.71 ± 0.20	8.3 ± 0.22	7.66 ± 0.2	8.4 ± 0.23	7.84 ± 0.2
415	8.5 ± 0.22	9.1 ± 0.24	9.76 ± 0.25	10.81 ± 0.28	10.05 ± 0.26	10.82 ± 0.29	10.31 ± 0.26
427	7.29 ± 0.19	8.15 ± 0.21	9.08 ± 0.24	10.48 ± 0.27	9.91 ± 0.25	10.66 ± 0.29	10.24 ± 0.26
439	4.27 ± 0.11	5.13 ± 0.14	6.06 ± 0.16	7.54 ± 0.2	7.42 ± 0.19	8.25 ± 0.22	8.05 ± 0.21
447						6.79 ± 0.18	6.76 ± 0.17
464						2.931 ± 0.081	3.091 ± 0.082

6.3 CHROMIUM (VI)

Chromium exists in two distinct chemical forms, the prevalence of which depends on concentration; one species dominates below approximately 0.2 g/L. The species have overlapping absorption spectra, which complicate the regression of the molar absorptivity curves. Only lower concentration samples were used to generate the regression curves below. The secondary species could not be refined, because the detector would saturate at concentrations where the species would be present.

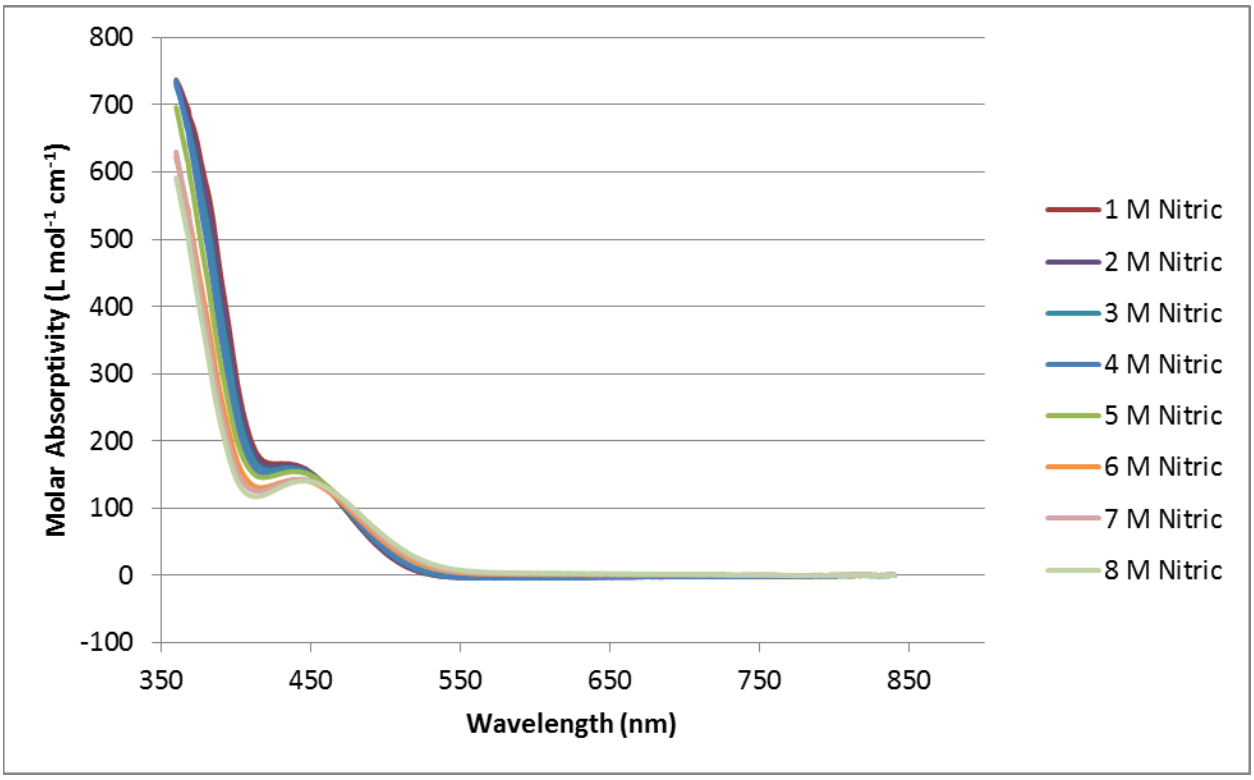

Figure 10—Chromium (VI) spectral data. Data were collected in 1-cm PMMA cuvettes in increasing concentrations of nitric acid.

Table 4—Molar absorptivity values (L mol^{-1} cm^{-1}) for Cr(VI) in 1–8 M HNO_3.

Wavelength (nm)	Nominal nitric acid concentration (molarity)							
	1	2	3	4	5	6	7	8
419	158 ± 17	156 ± 16	153 ± 23	150 ± 16	147 ± 22	142 ± 21	139 ± 21	131 ± 19
439	150 ± 16	148 ± 16	147 ± 22	145 ± 16	142 ± 21	140 ± 21	137 ± 21	132 ± 20
459	133 ± 14	131 ± 14	131 ± 20	129 ± 14	129 ± 19	126 ± 19	126 ± 19	124 ± 18
479	92 ± 9.7	91.6 ± 9.6	93 ± 14	92 ± 9.9	94 ± 14	93 ± 14	95 ± 14	96 ± 14
499	44.5 ± 4.7	45.2 ± 4.7	47.1 ± 7	48 ± 5.2	52.1 ± 7.7	52.9 ± 7.8	55.9 ± 8.4	58.4 ± 8.6
519	13.8 ± 1.5	14.7 ± 1.5	16.2 ± 2.4	17.4 ± 1.9	21.2 ± 3.1	22.6 ± 3.4	24.9 ± 3.7	27.3 ± 4

Underlined values are from a single dataset. All other values are the average of two separate experiments.

6.4 CHROMIUM (III)

The trivalent chromium species shows two large absorbance peaks. The errors on this particular dataset are higher than those in the rest of this study due to the use of an inappropriate pipettor that had a larger standard error. Because of this, it is hard to determine whether there is any distinction or trend in the peak values.

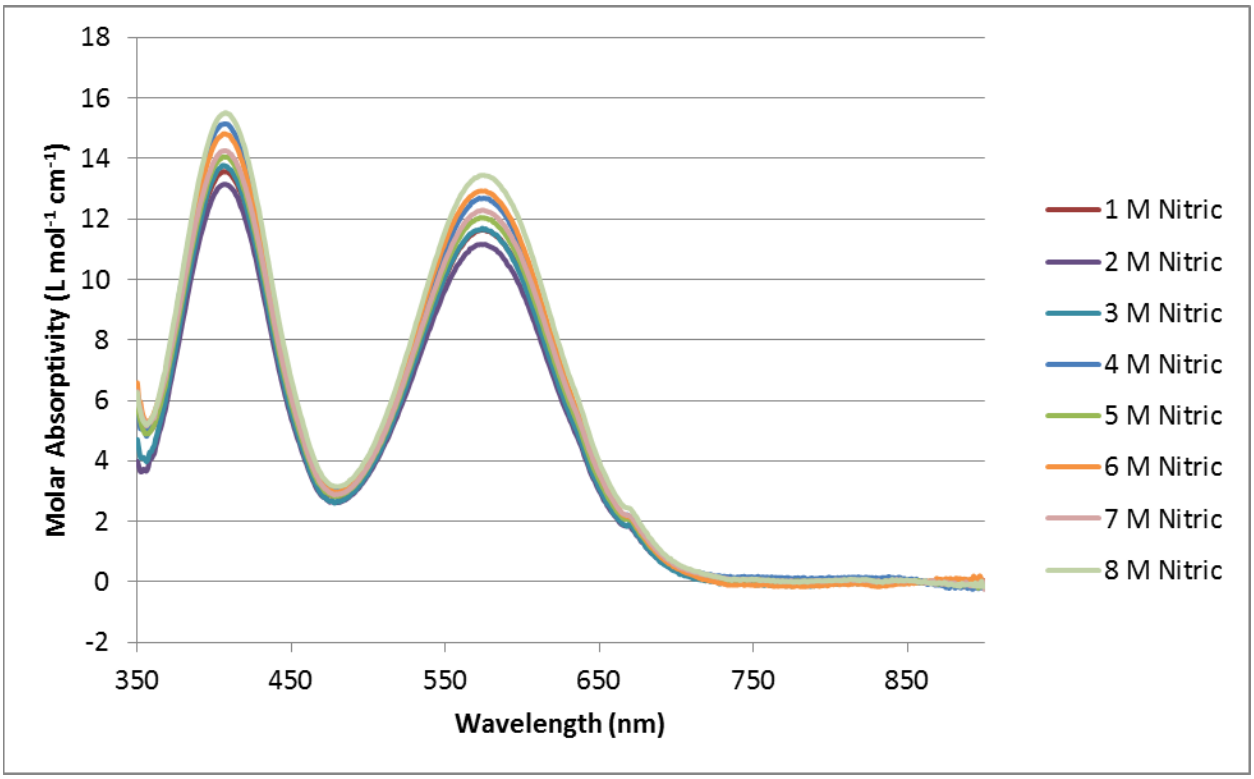

Figure 11—Chromium (III) spectral data. Data were collected in 1-cm PMMA cuvettes in increasing concentrations of nitric acid.

Table 5—Molar absorptivity values (L mol^{-1} cm^{-1}) for Cr(III) in 1–8 M HNO_3.

Wavelength (nm)	Nominal nitric acid concentration (molarity)							
	1	2	3	4	5	6	7	8
624	6.47 ± 0.65	6.2 ± 0.6	6.45 ± 0.63	6.92 ± 0.69	7.11 ± 0.71	7.36 ± 0.6	6.94 ± 0.72	7.87 ± 0.78
574	11.8 ± 1.2	11.1 ± 1.1	11.6 ± 1.1	12.3 ± 1.2	12.5 ± 1.3	13 ± 1.1	12.1 ± 1.3	13.4 ± 1.3
524	6.3 ± 0.64	6.13 ± 0.6	6.35 ± 0.62	6.69 ± 0.67	6.94 ± 0.69	7.22 ± 0.59	6.64 ± 0.69	7.4 ± 0.74
435	9.09 ± 0.92	8.67 ± 0.85	9.09 ± 0.89	9.8 ± 0.98	9.79 ± 0.98	9.84 ± 0.81	9.54 ± 0.98	10.5 ± 1
406	13.9 ± 1.4	13.1 ± 1.3	13.8 ± 1.3	14.8 ± 1.5	14.7 ± 1.5	14.7 ± 1.2	14.1 ± 1.5	15.3 ± 1.5
380	9.02 ± 0.91	8.72 ± 0.85	9.32 ± 0.91	10.2 ± 1	10.2 ± 1	10.07 ± 0.83	9.9 ± 1	10.7 ± 1.1

Underlined values are averaged from two datasets. All other values are the average of three separate experiments.

6.5 IRON (III)

Due to the low molar absorptivity coefficients for the trivalent iron system, several refined wavelengths could not be refined at low acid concentrations. The spectra show essentially continuum absorption below 450 nm. A small peak at approximately 410 nm is present at concentrations of nitric acid below 3 molar.

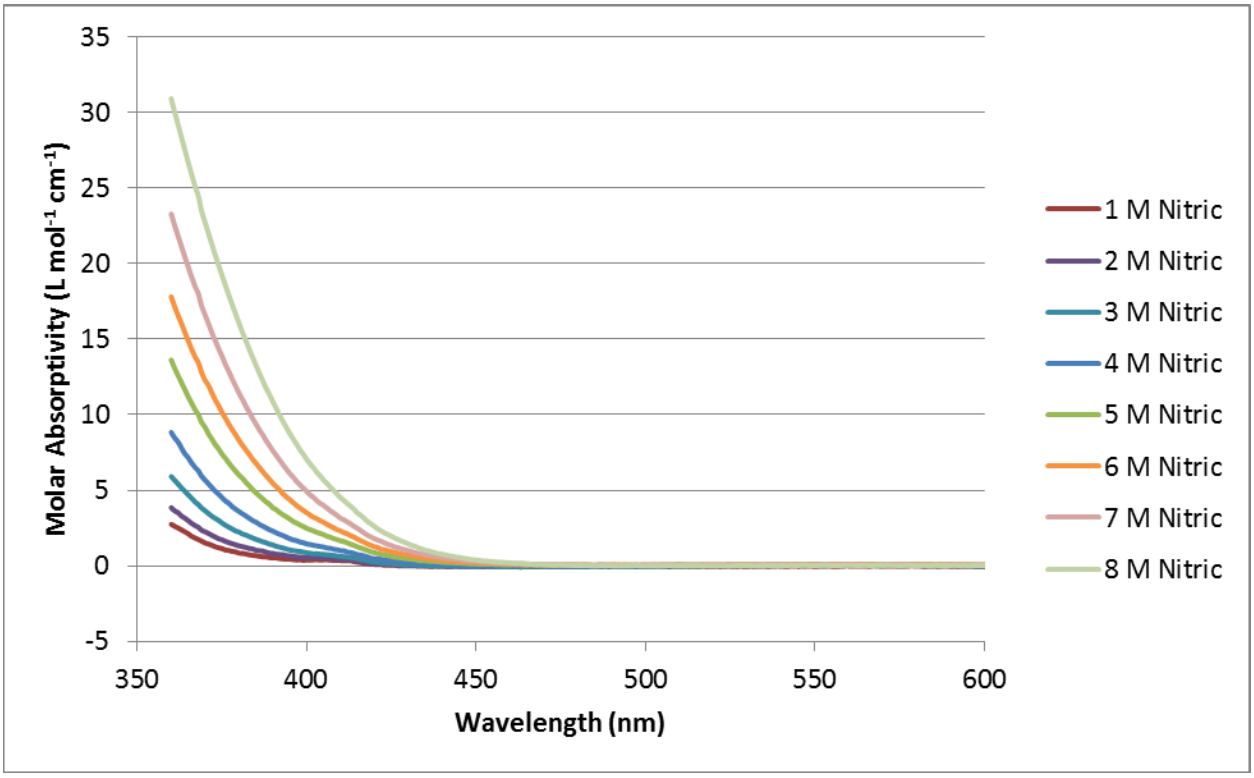

Figure 12—Iron (III) spectral data. Data were collected in 1-cm PMMA cuvettes in increasing concentrations of nitric acid.

Table 6—Molar absorptivity values (L mol^{-1} cm^{-1}) for Fe(III) in 1–8 M HNO_3.

Wavelength (nm)	Nominal nitric acid concentration (molarity)							
	1	2	3	4	5	6	7	8
370	1.547 ± 0.080	2.21 ± 0.16	3.55 ± 0.26	5.71 ± 0.41	9.10 ± 0.65	12.29 ± 0.88	16.8 ± 1.2	22.7 ± 1.6
380	0.837 ± 0.044	1.28 ± 0.10	2.04 ± 0.15	3.58 ± 0.26	5.88 ± 0.42	8.24 ± 0.59	11.41 ± 0.81	16.0 ± 1.1
390	0.522 ± 0.028	0.949 ± 0.099	1.28 ± 0.10	2.32 ± 0.17	3.74 ± 0.27	5.38 ± 0.38	7.56 ± 0.54	10.80 ± 0.77
400	0.0736 ± 0.0083	0.84 ± 0.14	0.843 ± 0.045	1.44 ± 0.10	2.38 ± 0.17	3.43 ± 0.25	4.85 ± 0.35	7.03 ± 0.50
410		0.503 ± 0.054	0.599 ± 0.032	1.015 ± 0.073	1.58 ± 0.11	2.22 ± 0.16	3.11 ± 0.22	4.51 ± 0.32
420		0.123 ± 0.012	0.251 ± 0.016	0.500 ± 0.038	0.846 ± 0.062	1.195 ± 0.086	1.77 ± 0.13	2.67 ± 0.19
430		0.0373 ± 0.0077	0.042 ± 0.011	0.264 ± 0.023	0.457 ± 0.035	0.665 ± 0.049	0.948 ± 0.069	1.55 ± 0.11
440				0.104 ± 0.014	0.247 ± 0.022	0.334 ± 0.027	0.510 ± 0.038	0.890 ± 0.066

Underlined values are from a single dataset. All other values are the average of two separate experiments.

6.6 NICKEL (II)

The nickel spectrum does not contain a non-absorbing region in the examined region (850–350 nm). Without a defined zero-absorbance point, drift in the spectrometer zero point becomes non-trivial. This required that an artificial zero point be defined; in this case the zero was defined as 500 nm. This will make this data collection less valuable for quantitative data analysis. The large observed variance in the nickel data is due to the low absorbance of the samples; the maximum absorbance for all samples was approximately 0.1 absorbance units. However, despite these deficiencies, with regard to H-Canyon work, the molar absorptivity coefficients are so small that they will not significantly influence any spectra collected at the concentration levels that could be reasonably expected to occur in the process tanks.

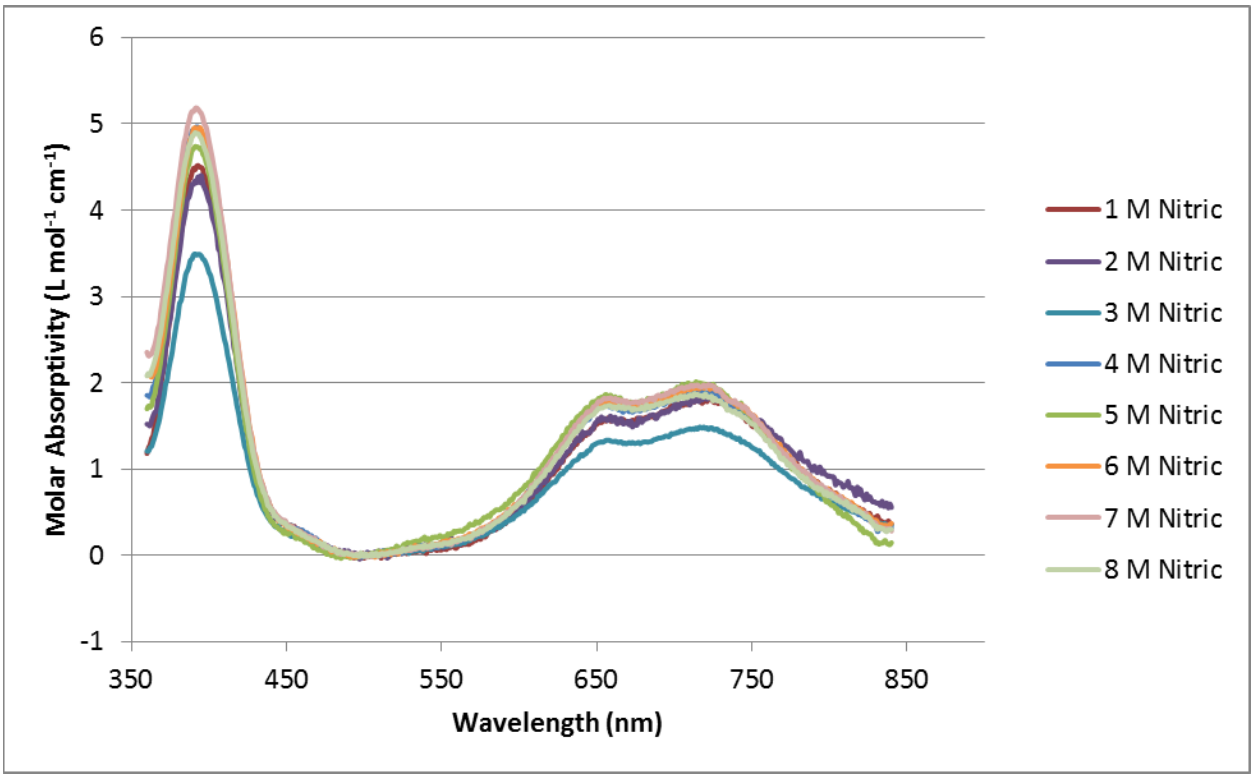

Figure 13—Nickel (II) spectral data. Data were collected in 1-cm PMMA cuvettes in increasing concentrations of nitric acid.

Table 7—Molar absorptivity values (L mol^{-1} cm^{-1}) for Ni(II) in 1–8 M HNO_3.

Wavelength (nm)	Nominal nitric acid concentration (molarity)							
	1	2	3	4	5	6	7	8
786	0.797 ± 0.044	1.077 ± 0.089	1.52 ± 0.14	0.998 ± 0.081	0.999 ± 0.084	0.906 ± 0.072	1.11 ± 0.14	0.852 ± 0.089
730	1.70 ± 0.13	1.99 ± 0.16	2.24 ± 0.19	1.90 ± 0.15	1.98 ± 0.16	1.86 ± 0.15	1.91 ± 0.20	1.72 ± 0.17
707	1.75 ± 0.14	2.01 ± 0.17	2.28 ± 0.19	1.93 ± 0.15	2.00 ± 0.21	1.95 ± 0.15	2.00 ± 0.21	1.78 ± 0.18
663	1.57 ± 0.12	1.77 ± 0.15	1.86 ± 0.15	1.76 ± 0.14	1.79 ± 0.14	1.82 ± 0.14	1.86 ± 0.19	1.67 ± 0.17
628	1.110 ± 0.087	1.28 ± 0.11	1.51 ± 0.13	1.28 ± 0.10	1.39 ± 0.11	1.32 ± 0.10	1.35 ± 0.14	1.21 ± 0.12
418	2.23 ± 0.17	2.46 ± 0.20	1.88 ± 0.15	2.40 ± 0.19	2.33 ± 0.19	2.37 ± 0.19	2.35 ± 0.24	2.28 ± 0.23
396	4.37 ± 0.34	4.82 ± 0.40	3.71 ± 0.28	4.82 ± 0.38	4.79 ± 0.38	4.84 ± 0.38	4.93 ± 0.50	4.57 ± 0.46

374	2.60 ± 0.20	2.94 ± 0.24	2.36 ± 0.20	3.22 ± 0.26	3.43 ± 0.28	3.32 ± 0.26	3.81 ± 0.40	3.17 ± 0.32

Italicized values are from a single dataset. All other values are the average of two separate experiments.

7 PROJECT SUMMARY

This project successfully advanced the ability to collect near-real-time information that can be used to safeguard operations of a nuclear reprocessing facility. By providing chemical, and concentration, information on process streams, the facility operator can gain valuable information on process performance, material in use, and chemical conditions. The basic system was developed with COTS materials to minimize cost, decrease system complexity, and increase the ability to repair/replace system components.

It should be noted that developing the interface between the spectrometer system and the facility infrastructure is a critical and facility-specific step. Each facility will have a slightly different operational plan and will require a custom interface. However, these interfaces can be made very robust with few consumable items. This methodology is compatible with canyon, hot cell, and glovebox based systems. More commercial reprocessing operations that utilize some form of passive, secure cell construction will require additional modifications at the planning stage to allow access to a process stream.

Both cells worked as expected once installed and correctly adjusted to the H-Canyon utilities. The micro flow cell was successfully used on at least five separate occasions over a 2-year span to monitor tank valence states. With the exception of the initial installation, the micro flow cell system was successfully calibrated and operated without consultation by Argonne staff. Although the loss of on-line, real-time monitoring data was unfortunate, the LPFC provides reasonable data when a stagnant solution is trapped in the cell. Both systems allow for the monitoring and tracking of materials at two extreme concentration profiles for safeguard-related measurements.

Finally, a high-fidelity spectroscopic datasets were generated for uranium, plutonium and transition metals commonly found in stainless steel. These datasets were generated using a new methodology written specifically for this project and analyzed using a novel code generated at Argonne for the evaluation of absorbance data via a maximum-likelihood estimation analysis. Both of these components could be widely used for other spectroscopic applications.

8 ACKNOWLEDGEMENTS

This project could not have been completed without the help and assistance of many employees at both H-Canyon and SRNL. The Argonne research staff would like to extend our deepest thanks to all who assisted us during this exciting venture. Special thanks are offered to Lindsay Sexton, Neil McIntosh, Pat O'Rourke, Robert Lascola, Brayden Brown, Michael Restivo, Jackie Cooper and for their commitment and dedication to this project.

9 REFERENCES

Klygin, A.E.; Kolyada, N.S.; Smirnova, A.E. Spectrophotometric investigation of complex formation in the uranyl nitrate - nitric acid - water system. *Zhurnal Neorganicheskoi Khimii (Russian Journal of Organic Chemistry)*. **1970**, 15, 1719–1721.

Lascola, R.; Livingston, R.R.; Sanders, M.A.; McCarty, J.E.; Dunning, J.L. Online Spectrophotometric Measurements of Uranium and Nitrate Concentrations of Process Solutions for Savannah River Site's H-Canyon. *Journal of Process Analytical Chemistry*. **2002**, 7(1), 14–20.

Lee, M.H.; Park, Y.J.; Kim, W.H. Absorption spectroscopic properties for Pu (III, IV and VI) in nitric and hydrochloric acid media. *Journal of Radioanalytical and Nuclear Chemistry*. **2007,** 273 (2), 375–382

Nash, C.A. *Literature review for oxalate oxidation processes and plutonium oxalate stability*; SRNL-STI-2012-00003; Savannah River National Laboratory: Aiken, South Carolina, 2012.

Smith, N.A. Speciation and spectroscopy of the uranyl and tetravalent plutonium nitrate systems: Fundamental studies and applications to used fuel reprocessing. Ph.D. dissertation, University of Nevada, Las Vegas, Las Vegas, NV, 2010.

Smith, N.A.; Krebs, J.F.; Hebden, A.S. Scientific data supporting *UV-Vis Spectroscopy as a Tool for Safeguards; Instrumentation installation and fundamental data collection*; ANL/NE-15/7; Argonne National Laboratory: Argonne, IL, 2015. https://anl.app.box.com/APT120663-ANL-NE-15-7

Thomas, O.; Burgess, C. *UV-visible Spectrophotometry of Water and Wastewater*; Elsevier; the Netherlands, 2007.

Wilson, R.E.; Hu, Y.J.; Nitsche, H. Detection and Quantification of Pu(III, IV, V, and VI) Using a 1.0-Meter Liquid Core Waveguide. *Radiochimica Acta*. **2005,** *93*, 203–206.

APPENDIX A
ANNOTATED BIBLIOGRAPHY

INTRODUCTION

To more narrowly focus the scope the following definitions were used: (1) in-line, measurements made within the process on the flowing streams; (2) on-line, measurements on a fraction of the total stream, as for example on a by-pass stream; (3) at-line, measurements on samples physically taken from the stream and immediately analyzed at the site; and (4) off-line, measurements on samples removed and sent to a laboratory for analysis.[1] Thus, this annotated bibliography focuses on in-line/on-line monitoring techniques employing ultraviolet-visible (UV-vis) methods developed for monitoring actinides in process streams. There are also several references to Applied Technology reports that were not included in this bibliography. The references have been organized chronologically. It should be noted that the Argonne team is aware of two earlier references to the use of on-line spectrophotometry of uranium solutions for process monitoring and control.

CARSON, W.N.; MICHELSON, C.E. "AN AUTOMATIC PHOTOMETER" HW-27744; HANFORD ATOMIC PRODUCTS OPERATION: HANFORD, WA, 1953; 17 PP.

CARSON, W.N.; VAN METER, W.P.; MICHELSON, C.E., "IN-LINE ANALYSIS OF METAL RECOVERY PROCESS FEED." HW-29751; HANFORD ATOMIC PRODUCTS OPERATION: HANFORD, WA, 1953.

SCOTT, F.A.; VAN METER, W.P. "THE DESIGN AND CONSTRUCTION OF AN IN-LINE PHOTOMETER SENSING UNIT" HW-39926; HANFORD ATOMIC PRODUCTS OPERATION: HANFORD, WA, 1955; 26 PP.

The authors note the “considerable” need for the continuous monitoring of PUREX plant streams for uranium in the concentration range of 0.1–1.5 M for purposes of process control. The authors state that the report describes the continuation of the work of Carson, Van Meter, and Michelson on the application of light photometry to the in-line determination of uranium. In-line measurements in the plant have determined the uranium concentration of plant streams to within ±6% of the concentrations reported by the laboratory. The authors attributed the differences between the on-line and laboratory values as being due to the instability of the standards used for calibration. A separate measurement of the turbidity is used to compensate for large amounts of turbidity in process streams. Suitable correction factors to compensate for organic phase

[1] Babcock, S.M.; Feldman, M.J. ; Wymer, R.G.; Hoffman, D. “Workshop on Instrumentation and Analyses for A Nuclear Fuel Reprocessing Hot Pilot Plant” CONF-8005121; Oak Ridge National Laboratory: 1980; 26pp.

degradation products were obtained by measuring the light absorption of uranium-free solvent at another point in the process. The report offers an extensive description of the hardware used in the on-line spectrophotometer.

SCOTT, F.A. "AN ANALYSIS OF THE IN-LINE URANIUM PHOTOMETER DATA FROM PUREX HOT SEMI-WORKS RUNS PX-2 THROUGH PX-9" HW-40313; HANFORD ATOMIC PRODUCTS OPERATION: HANFORD, WA, 1955; 26 PP.

The fourth reference describes operation of in-line uranium photometers on three organic and two aqueous streams in the PUREX hot semi-works for eight runs. It is reported that U concentrations indicated by the photometers agree with those given by laboratory analysis. However, differences between the two analyses can be as much as 9%. The readings from the photometers on the organic streams were corrected for solution turbidity effects based on measurements from a separate turbidity cell. Another photometer is used to monitor the recycled organic solvent to correct for solvent effects. No mention is made of correcting the aqueous phase for effects to changing HNO_3 concentrations. The report also mentions a secondary source of divergence, between photometer and laboratory results, due to frequent erratic results from the photometers. The source of the erratic behavior was not identified in the report. Thirteen figures present data.

PROHASKA, C.A. “A FLOW COLORIMETER FOR MEASURING URANIUM CONCENTRATION IN PROCESS STREAMS” DP-229; SAVANNAH RIVER LABORATORY: 1957; 21 PP.

A flow colorimeter, to measure uranium concentrations continuously, was developed as part of a program to provide analytical instrumentation for control of separations processes. The unit was designed to operate with either aqueous or organic streams. Aqueous solutions with uranium concentrations of 45–55 g U/L were measured in the laboratory with a precision of ±1%. The unit was put into service and operated satisfactorily for 4 months in the Metal Recovery Plant at Oak Ridge National Laboratory (ORNL), where it was used to measure concentrations between 26 and 36 g U/L and between 45 and 55 g U/L. The estimated precision during the plant service test was ±3%. In both plant and laboratory service, the instrument variation and drift over a 24-hour period were equivalent to a change of uranium concentration of less than ±1 g U/L. The unit offers correction for phenomena such as turbidity, window fouling or darkening, and changes in light source intensity. The author notes that an unsuccessful attempt was made to correlate the colorimeter chart reading with the laboratory analysis of grab samples. The discrepancy between the instrument and laboratory results was attributed to time lag between a reading and grab sample time stamp. Overall, the colorimeter reading agreed well with the grab sample analysis within ±3 g U/L, and usually within ±1 g U/L.

LANDRY, J.W. “INLINE INSTRUMENTATION: GAMMA MONITOR, URANIUM COLORIMETER” ORNL-2978; OAK RIDGE NATIONAL LABORATORY: 1960; 26 PP.

The report describes testing and modification of the uranium colorimeter, developed at Savannah River Laboratory (SRNL), at ORNL. Testing of the SRNL on-line uranium

spectrophotometer at the ORNL Metal Recovery Plant occurred over a 1-year period. To compensate for the presence of organic phase degradation products in the organic stream, a three-cell colorimeter was designed in which the solvent passes through cells before and after it extracts the uranium. The three-cell in-line colorimeter was built by the ORNL Inline Instrumentation Group. The report also describes the in-line gamma monitors, developed by ORNL, used at the ORNL pilot plants.

COLVIN, D.W. "A COLORIMETER FOR IN-LINE ANALYSIS OF URANIUM AND PLUTONIUM SOLUTIONS" DP-461 ; SAVANNAH RIVER LABORATORY: 1960; 25 PP.

A colorimeter is described that can be used to monitor aqueous process solutions continuously for uranyl nitrate or plutonium nitrate concentration. The instrument was tested under plant conditions in the concentration range from 0.1 to 70 g U/L and 0.1 to 10 g Pu/L. The instrument error was stated as being ±1% of the span, but errors of 15 to 20% can be caused by other variables such as acidity and other salts present. A pulsating light source was used resulting in the instrument being unaffected by changes in phototube dark current. The sample cell was designed for in-line installation. A procedure was developed for recalibrating the instrument after installation on a process stream. In-line recalibration involved diverting the light beam around the sample cell. The author states that the precision and accuracy of the measurements were found to be limited by the effect of other variables in the solutions rather than instrument noise or calibration drift. Temperature effects were determined at 28, 40, and 50°C. Effects of turbidity were determined by adding organic solvent to the uranyl nitrate solutions. The resulting change in the uranium measurement was a maximum of about 5%. The effect of the organic solvent was reduced to less than 1% by installing a separator-degasser in the inlet sample line. The author noted, correctly, that when nitric acid is present in a uranyl nitrate solution an accurate measurement cannot be obtained unless the acid concentration is held relatively constant and the instrument is calibrated with solutions that contain the normal acid concentration.

BOSTICK, D.T. "THE SIMULTANEOUS ANALYSIS OF URANIUM AND NITRATE" ORNL-TM-6292; OAK RIDGE NATIONAL LABORATORY: 1978; 40 PP.

BOSTICK, D.T. "ACID COMPENSATED MULTIWAVELENGTH DETERMINATION OF URANIUM IN PROCESS STREAMS” CONF-791117-22; OAK RIDGE NATIONAL LAB: 1979; 8 PP.

BOSTICK, D.T. "ACID-COMPENSATED MULTIWAVELENGTH DETERMINATION OF URANIUM IN PROCESS STREAMS" IN MEASUREMENT TECHNOLOGY FOR SAFEGUARDS AND MATERIALS CONTROL - PROCEEDINGS FROM AMERICAN NUCLEAR SOCIETY TOPICAL MEETING, NATIONAL BUREAU OF STANDARDS SPECIAL PUBLICATION NO. 582, THOMAS R. CANADA AND B. STEPHEN CARPENTER, EDS.; KIAWAH ISLAND, SOUTH CAROLINA, NOV. 26-30, 1979; NATIONAL BUREAU OF STANDARDS: 1980; 121–128.

A direct spectrophotometric method has been developed for the determination of 20–200 g U/L in the presence of 3–5 M nitric acid. The calculated relative standard deviation of uranium and nitrate concentrations was 5.4% and 15.5%, respectively. The photometric procedure is slightly affected by temperature with an overestimation of uranium concentration of 0.2 g U/L·°C. The authors note that earlier techniques were subject to errors as great as 15–20% due to variations in nitric acid concentration and temperature, in addition to turbidity. The authors reported four major absorption maxima, occurring at 426, 416, 403, and 359 nm. The 416-nm absorption line possessed the greatest sensitivity to U concentration at constant HNO_3, whereas the 359-nm line exhibited limited sensitivity to HNO_3. The absorption at all wavelengths increases with nitric acid concentration. It was reported that the accuracy of the U monitor should not be significantly altered by the slight absorbance changes that occur within the acidity range studied. The precision and accuracy in the simultaneous analysis of uranium and nitrate were compared using combinations of two of the four maxima. The precision in calculating U was found to be best if the analysis was based on either 416 nm/426 nm or 426 nm/403 nm data. The 416 nm/426 nm data that exhibited the greatest sensitivity, for both uranium and nitrate, were selected for use in the uranium monitor. It was reported that the nitrate analysis is not as accurate or precise as that obtained for uranium. The accuracy of the nitrate analysis is best if based on 416 nm/426 nm data.

BOSTICK, D.T.; STRAIN, J.E. "EXPERIMENTAL PARAMETERS IN THE PHOTOMETRIC ANALYSIS OF URANIUM IN TBP-DODECANE SOLUTIONS" ORNL/TM-7551; OAK RIDGE NATIONAL LABORATORY: 1981; 27 PP.

A systematic study of the direct colorimetric determination of uranium in tributyl phosphate-dodecane solutions was made. The authors investigated the influence of a number of parameters on the accuracy of uranium analysis by UV-vis spectrophotometry. The parameters included concentrations of HNO_3, tri-butyl phosphate (TBP), mono- and dibutyl phosphate concentrations, temperature, and extent of solvent degradation. The authors also noted that absorbance from solvent coloration, produced by the presence of TBP nitrification products, must be subtracted from the total 416-nm absorbance in order to obtain an accurate analysis of U under process conditions. The operating range of the procedure, using a 0.5-cm photometric cell, was 1 to 100 g U/L, with an estimated accuracy of ±0.5 g U/L. Instrument redundancy would also simplify fabrication, maintenance, and calibration requirements for uranium detection in the reprocessing facility.

VAN HARE, D.R.; PRATHER, W.S.; BOYCE, D.A.; SPENCER, W.A. "ONLINE FIBER-OPTIC PHOTOMETER" DP-MS-85-127; SAVANNAH RIVER LABORATORY: 1985; 19 PP.

At the time of the instrument development, the Savannah River Plant was producing plutonium-238 heat sources. In the process neptunium and plutonium, both in +4 oxidation state, are separated from other elements, precipitated, and converted to an oxide form. Six of the photometers were installed at SRP to monitor the elution of neptunium or plutonium from anion exchange columns. The Np or Pu in a 7–8 M HNO_3 solution is loaded onto an anion exchange column and then eluted using 0.2 M HNO_3 as a concentrated plug of solution. During elution of

Np and Pu valves must be switched to obtain the greatest portion of the Gaussian shaped elution band, thereby maximizing the concentration of collected product. The authors state that a multiple fiber bundle was chosen instead of a larger diameter single fiber because it carried more light to the phototubes, increasing the dynamic range of the photometer. No process data were presented.

MOSER, D.R.; KLATT, L.N. "APPLICATION OF IN-LINE PHOTOMETER TO SOLVENT EXTRACTION PROCESS CONTROL" CONF-860754-2; OAK RIDGE NATIONAL LABORATORY: 1986; 28 PP.

Short summary and slides presented at the Joint United Kingdom and United States Technical Symposium on Control and Instrumentation (July 29–31, 1986, Harwell, England). A multi-wavelength, multichannel photometer, using fiber optic probes, was designed and was applied to solvent extraction process control. The instrument was used for automatic control of a centrifugal contactor bank (extraction mode, uranium only); pulsed column (stripping mode, uranium only); and mixer-settler (co-extraction mode, irradiated fuel) were reported as having been successfully demonstrated.

O'ROURKE, P.E.; VAN HARE, D.R. "ONLINE FIBER-OPTIC SPECTROPHOTOMETRY" DP-MS-87-100; SAVANNAH RIVER LABORATORY: 1987; 33 PP.

The report describes a multiplexed fiber-optic light transmission system that connects six process sample locations to a single spectrophotometer that is up to 100 m away from the monitoring points. Fiber optics are used to transmit UV-vis signals to the diode array spectrophotometer that collects the absorption spectra in the range of 300 to 820 nm. Reported absorption data from a sample location is calculated from many individual spectra. Each spectrum is tested for baseline offset before it is included in average and variance calculations. The authors note that averaging reduces noise, and the variance is used to indicate the presence or absence of flow through the sample cell. They also note that the spectral variance is significantly higher in flowing streams than in static streams. The absorption data are reduced to analyte concentrations and residual data using a multivariate model of the absorption characteristics of the chemical system. Importantly, it was noted that it was not possible to correct errors in analyte concentrations due to unknown effects, but that the residual data can be used to indicate when substantial errors may be present. The report provides an excellent description of the hardware and software used in the system. Because the samplers at the Savannah River Plant operate like an air lift pump, a sampler interface incorporating a degasser was required to introduce a bubble-free stream into the process flow cell. Second derivative spectra were used to build the models for the actinide concentrations. The second derivative models were reported as being insensitive to spectral baseline shifts, and less sensitive to particle scattering and monotonic spectral interferences. Models were constructed for the nitrate systems of UO_2^{2+}, Pu^{3+}, and Pu^{4+}. The first online fiber-optic spectrophotometer system was installed on a full-scale prototype ion-exchange system designed to extract uranyl ions from 0.1 M nitric acid. The ion-exchange system consisted of a uranyl nitrate feed tank and pump and two 6-inch-diameter, 20-foot-long ion-exchange columns arranged in series. In a second installation of the system, 68 hours of uranyl concentration data are shown from a test involving a uranyl nitrate

tank air lift sampler. A third installation was on an air lift tank sampler to measure the Pu^{3+} concentration in a product recycle tank. The report includes data of the concentrating effect from evaporation on the Pu^{3+} solution in this tank over time.

VAN HARE, D.R.; O'ROURKE, P.E.; PRATHER, W.S. "ONLINE FIBER OPTIC SPECTROPHOTOMETRY" DP-MS-88-186; SAVANNAH RIVER LABORATORY: 1988; 44 PP.

A fiber-optic diode array process analyzer developed and installed in a radiochemical separations facility at the Savannah River Plant is described. The analyzer monitors the uranium and nitrate concentration of seven aqueous process streams in the second uranium cycle purification process. The process flow cells were simply Swagelok 1/2-inch unions, crosses, and tees. Due to the two-phase (air/liquid) nature of the solution being sampled, a sampler interface incorporating a degasser was required to introduce a bubble-free stream into the flow cell. The analysis software was developed by the authors and with partial least squares (PLS), principle component regression (PCR), classical least squares (CLS), and multiple linear regression (MLR) analysis models. The authors used second derivative spectra to build models for the uranium concentration as they were insensitive to spectral baseline shifts, and less sensitive to particle scattering and monotonic spectral interferences. Uranyl nitrate models describe uranyl concentrations between 0.2 and 20 g U/L, and nitrate concentrations between 0.1 and 8 M. Accuracy of the online data was determined by comparison to laboratory measurement of manual samples. The authors state that the accuracy of the laboratory method was ±2%, but then inferred that the accuracy of the online spectrophotometer was at least ±2%, "since the online and laboratory results generally agree to within the accuracy of the laboratory method."

BALDWIN, D.L.; STROMATT R.W. "PLUTONIUM, URANIUM, NITRATE MEASUREMENTS IN PUREX PROCESS STREAM BY REMOTE FIBER OPTIC DIODE ARRAY SPECTROPHOTOMETRY" PNL-SA-15318; PACIFIC NORTHWEST LABORATORY: 1988; 17 PP.

The authors state that the focus of the work at Pacific Northwest Laboratory (PNNL) was to apply the foundation of on-line measurement work performed at Savannah River Laboratory to the development of technology for PUREX plant process chemistry with initial focus on the Pu strip feed. In the Pu strip feed, Pu^{4+} concentrations of 10 to 50 g/L are expected with Pu^{3+} and Pu^{6+} being up to one-tenth that level. The authors state that these concentrations are much higher than those at the Savannah River Plant. Nitrate concentrations of 1 to 3 M were expected which are considerably lower than at the SRP at the time. Much of the equipment and techniques used by PNL are similar to those developed at SRL.

DAY, R.S.; VIGIL, A.R.; MARSH, S.F. "A VISIBLE/NEAR-IR SPECTRAL DATABASE FOR PLUTONIUM SOLUTIONS OF KNOWN NITRIC ACID, FLUORIDE, AND OXALATE COMPOSITION" LA-11480; LOS ALAMOS NATIONAL LABORATORY: 1989; 23 PP.

Spectra of 126 solutions that contained known concentrations of plutonium, fluoride, oxalate, and nitric acid were acquired as a database for on-line spectrophotometry. This reference

has 15 figures each for 2 g Pu/L or 10 g Pu/L with varying concentrations of HNO_3 with fluoride or oxalate. Unfortunately, the results are not tabulated, nor are molar extinction coefficients reported.

BÜRCK, J. "SPECTROPHOTOMETRIC DETERMINATION OF URANIUM AND NITRIC ACID BY APPLYING PARTIAL LEAST-SQUARES REGRESSION TO URANIUM(VI) ABSORPTION SPECTRA" ANALYTICA CHIMICA ACTA, 254 (1991) 159–165.

The author notes that most of the spectrophotometric methods for U(VI) determination that had been developed involved uni- or bivariate calibrations. As they take the absorbance values at one or two wavelengths for calculating the U(VI) concentration. The author applies the method of PLS regression to the full spectra of appropriate U(VI)-HNO_3 solutions to more accurately predict the concentrations of both constituents. The PLS models for U(VI) and nitric acid were developed from a 32-sample calibration set. For the U model, the first latent variable corresponded to 98.75% of the spectral response and to 95.91% of the U(VI) variance. For HNO_3 only 7.56% of the variance was described by the first factor. Even after five latent variables, only ≈77% of the explained variance is reached. The author found that good prediction results for HNO_3 could be obtained if the spectral response matrix was pre-linearized. Using this revised model, the first latent variable describes 96.46% of the variance in HNO_3 concentration. This revised model is inferior to the original PLS model for predicting U(VI) concentrations, because less spectral variation is available to model uranium. The author states that one should use two models to predict U(VI) and HNO_3 concentrations in unknown samples, a four latent variable model using the original U(VI) spectra to predict U(VI) concentration, and a five latent variable model based on normalized spectra to predict nitric acid concentration.

KUNO, Y.; KAWABE, K.; AKIYAMA, T. “DEVELOPMENT OF AUTOMATIC SYSTEM FOR DETERMINATION OF U(IV), U(VI), PU(III), PU(IV), PU(VI) AND NITRIC ACID IN NUCLEAR FUEL REPROCESSING STREAMS BY SPECTROPHOTOMETRY” BUNSEKI KAGAKU, 1991, 40, T113–T118.

The authors developed and tested a UV-vis fiber optic system at the Tokai Reprocessing Plant. The method used experimentally collected spectra of U and Pu in each of their valence states [U(IV), U(VI), Pu(III), Pu(IV), and Pu(VI)] at various HNO_3 concentrations. The combinations of the individual spectra, chosen based on characteristics peaks for each oxidation state, were combined iteratively to compose a combined spectrum that matched the solution spectrum of the process stream. Data were collected with fiber-optic systems attached to a 10-mm path length cell. The ranges used were 0.7–20 g U^{4+}/L, 1.4–60 g U^{6+}/L, 0.3–8 g Pu^{3+}/L, 0.1–6 g Pu^{4+}/L, and 0.05–2 g Pu^{6+}/L. The method was limited to the HNO_3 concentration range of 0.5–5.5M. The analysis method was reported as being fully automated.

LASCOLA, R.; LIVINGSTON, R.R.; SANDERS, M.A.; MCCARTY, J.E.; DUNNING, J.L. "ONLINE SPECTROPHOTOMETRIC MEASUREMENTS OF URANIUM AND NITRATE CONCENTRATIONS OF PROCESS SOLUTIONS FOR SAVANNAH RIVER SITE'S H-CANYON" WSRC-MS-2001-00019; SAVANNAH RIVER SITE: 2001; 11 PP.

The authors state that this work builds upon pioneering efforts of Van Hare and O'Rourke carried out at the SRS in the late 1980s. The authors installed an online fiber-optic-based analyzer that uses a multiplexer and diode array spectrometer to rapidly acquire absorption spectra at multiple process locations within H-canyon operations. The authors focused their report on the operations at the H-canyon second uranium cycle. The spectrophotometers of Van Hare and O'Rourke were abandoned when the site's mission was redefined after the end of the Cold War. The instrument controls were located in the H-canyon control room. This on-line system relied on aspiration of process solution aliquots into a vial with a rubber septum. Excess solution was allowed to flow into the body of the flow cell that was constructed from a standard 1/2-inch stainless steel compression fitting union tee. Use of a union tee was flawed, because the solution entered and exited through the middle arm of the tee. This was observed during displacement of a highly concentrated uranium/nitric acid solution (d = 1.37 g/mL) by a more dilute solution (d = 1.16 g/mL), which required several hours. The authors reported that another factor governing sample exchange was the amount of air entrained in the sample. It was noted that too much air adversely affects the spectra taken through the flow cell, since air bubbles scatter light, increasing the baseline, and exclude solution, decreasing the effective path length. The calibration range used was 0–11 g/L U and 0.05–6 M nitrate as HNO_3. The authors developed models with root-mean-square validation errors of 0.08 g/L for uranium and 0.10 M for nitrate over a temperature range of 20–45°C. The process results were compared to laboratory results and are reported to be generally within the 95% confidence limits for both uranium (0.16 g/L) and nitrate (0.20 M).

LASCOLA, R.J.; LIVINGSTON, R.R.; SANDERS, M.A.; MCCARTY, J.E.; COOPER, G.A. "ON LINE SPECTROPHOTOMETRIC MEASUREMENT OF URANIUM AND NITRATE IN H CANYON" WSRC-TR-2002-00334; SAVANNAH RIVER SITE: 2002; 71 PP.

This is a review report describing the work by the Analytical Development Section. Two UV-vis fiber-optic spectrophotometry systems were developed to analyze a total of nine tanks. The acquired spectra were interpreted using PLS models that were valid for solutions with uranium concentrations up to 11 g/L and nitrate concentrations as high as 6 M. Concentration-dependent measurement uncertainties (2σ) are less than 0.30 g/L for uranium and 0.32 M for nitrate. The models incorporated corrections for the spectral effects of <3 g /L Fe and <1 g /L Hg. The total instrument consisted of two spectrophotometers operating in parallel. The instruments operated at uranium concentrations between 0 and 11 g/L and nitrate concentrations between 0.05 and 6 M at 20–45°C. The authors state that the temperature range does not represent the temperature of the solution in the tank. The solution temperature will equilibrate with the building temperature as the solution travels through the pipes from the tanks to the flow cells. The concentration-dependent uncertainty was between 0.10 and 0.30 g/L (2σ) for U and 0.18and 0.32 M (2σ) for NO_3^-. It was noted that the instrument was not designed to measure

waste streams in the highly enriched uranium (HEU) process. These streams—1AW, 1DW, 1BP, HAW bottoms, and LAW bottoms—are commonly characterized by low U concentrations (0.1–100 mg/L), substantial iron concentrations (typically 1–4 g/L, but up to 30 g/L in LAW bottoms), and potentially significant concentrations of other actinides. The combination of high Fe and low U concentrations makes U analysis by diode array spectroscopy nearly impossible. The previous problem of using process water to flush a dense solution (approximately 6 M nitric acid) from the flow cell over a period of several hours was addressed. The problem occurred because the solution entry tube extended only a short distance into the tee union, and the water did not enter the flow cell with enough force to displace the heavier solution at the bottom of the tee. The time required for flushing the cell was reduced to 2–3 minutes by extending the solution entry tube to a point just above the top of the optical path defined by the collimating lenses. This report also addressed the impact on dose rates to workers. It was concluded from model studies that on-line measurements would decrease the overall exposure of sample aisle operators and laboratory technicians, because fewer samplers will be collected and analyzed off-line. The report also addresses operation of the software used to perform data analysis.

LASCOLA R.J.; COOPER, G.A. "FEASIBILITY OF URANIUM CONCENTRATION MEASUREMENTS FOR H CANYON TANK 16.7" WSRC-TR-2002-00568; SAVANNAH RIVER SITE: 2002; 16 PP.

UV-vis spectrophotometers installed in H-Canyon were being used to monitor uranium and nitrate concentrations in nine tanks in the First and Second Uranium Cycles. The goal was to extend the system to include measurements of uranium in Tank 16.7, which receives the 1DW stream before it is sent to low activity waste. The H-Canyon spectrometer uses chemometric prediction models to reduce or eliminate the effects of chemical interferences and solution conditions. It was noted that the longer path length required for lower concentrations increases the sensitivity of the measurement, but that it also increases the effect of interfering species such as Fe. The new calibration solutions had uranium concentrations of 0.05, 0.10, 0.20, 0.40, 0.60, 0.80, and 1.0 g/L. Two uranium-free test solutions were also made containing 0.2 and 1.0 g/L Fe^{3+}. It was determined that a cell with a path length of 2.54 cm was sufficient. An alternative cell with a 5.08 cm path length, achieved by incorporating a retro-reflection design into the flow cell, was proposed but ultimately not used. There was a total uncertainty of 0.18 g/L for 0.5 g/L U, and 0.32 g/L for 1 g/L U, with a limit of quantitation of 0.15 g/L.

BRYAN, S.A.; LEVITSKAIA, T.G. “MONITORING AND CONTROL OF UREX RADIOCHEMICAL PROCESSES” IN ADVANCED NUCLEAR FUEL CYCLES AND SYSTEMS (GLOBAL 2007), BOISE, IDAHO (UNITED STATES), 9–13 SEP 2007; AMERICAN NUCLEAR SOCIETY: LA GRANGE PARK, IL, 2007; 176–179.

The objective of the project was to use a system of flow, chemical composition, and physical property measurement techniques for developing on-line real-time monitoring systems for the UREX process streams. The proposed system adds a UV-vis–near-infrared (NIR) spectrophotometer to a Raman spectrometer with a Coriolis meter and a conductivity probe previously developed by the authors. The authors listed the following Raman active species: (1) metal oxide ions, such as uranyl, neptunyl, and pertechnetate ions; (2) organics, such as

dodecane diluent, TBP, chlorinated cobalt dicarbolide (CCD), acetohydroxamic acid, diethylenetriamine pentaacetate (DTPA), lactic acid, as well as their degradation products; and (3) inorganic oxoanions and water. The UV-vis-NIR spectrophotometer would monitor trivalent and tetravalent actinides and lanthanides in both aqueous and organic phases. Both spectrometer systems used fiber-optic probe technologies. No in-process demonstrations were presented. However, the system without UV-vis-NIR capability was used to measure the concentration of components of solutions of high brine/high alkalinity wastes during retrieval from Hanford waste storage tanks. The authors did incorrectly note that research on instrumentation for the on-line control of nuclear fuel reprocessing streams dated to the 1970s. As shown in this annotated bibliography, interest in on-line control of nuclear fuel reprocessing streams dates to at least the mid-1950s.

LASCOLA, R.; SHARMA, V. "APPLICATION OF ABSORPTION SPECTROSCOPY TO ACTINIDE PROCESS ANALYSIS AND MONITORING" SRNL-STI-2010-00338; SAVANNAH RIVER NATIONAL LABORATORY: 2010; 3 PP.

This report describes the installation of a spectrophotometer to measure plutonium concentration in the range of 0.1–1.5 grams/liter (g/L) in the high concentration cut from an anion exchange column, during which nitric acid concentration decreases rapidly from 8 M to 2 M. As expected, the Pu remains in the +4 oxidation state with the absorption spectrum changing due to the varying distribution of Pu–NO_3 complexes. It was stated that a customized filter was required because commercially available filters near the strong 475 nm band do not accommodate the spectral variation. The authors also describe the simultaneous measurement of UO_2^{2+} and Pu^{3+} in solutions from spent fuel processing. Plutonium directly interferes with U absorption in the 390–440 nm range and can be present in tenfold excess. In addition, small amounts of metallic cations present from the dissolved starting material can overlap spectrally with both U and Pu. Simultaneous measurement of U and Pu was achieved through PLS analysis of absorption spectra. The accuracy of the measurement appears to be constant for $[Pu^{3+}]/[UO_2^{2+}] \leq 4$. At $[Pu^{3+}]/[UO_2^{2+}] > 4$, the absorbance due to Pu (0.45) is 11 times the absorbance of U (0.04).

APPENDIX B
METHODOLOGY

METHODOLOGY FOR COLLECTION OF MOLAR ABSORPTIVITY COEFFICIENTS UNDER HIGH ACID CONDITIONS

Applicable to *d* and *f* block elements with UV-Visible absorption bands in mineral acids

B.1 INTRODUCTION

The collection of ultraviolet, visible, or near-infrared absorbance spectroscopy (UV-vis or UV-vis-NIR) data is useful for many applications including basic research, pharmaceutical synthesis, and elemental analysis. However, the value of this data is dependent on the analyst's ability to discern relevant chemical information from the absorbance data. A fundamental use of UV-vis spectroscopy is to measure the concentration of an absorbent species. To do this, three parameters must be known or measured: the absorbance of the solution, the path length of the cell, and the molar absorptivity of the species. The molar absorptivity is specific to a particular chemical species and, as such, may change as the solution conditions change. For example, as the solution around the Fe^{3+} moves from a basic to an acidic environment, the speciation of Fe^{3+} complexes shifts from one dominated by hydroxyl species [e.g., $Fe(OH)_3$] to neutral *aquo* species to acid conjugates [e.g., $FeCl_2^+$, $Fe(NO_3)_3$], the absorbance of the species will vary accordingly. Therefore, any study of molar absorptivity constants must pay particular attention to the environment surrounding the analyte (i.e., concentrations of ligands or coordinating molecules). If modeling techniques and spectroscopy are combined, species-specific molar absorptivity values can be reported under the conditions stated.

For systems where the speciation of the system cannot be known or predicted, an empirical study must be performed instead. These situations arise when there is either a lack of systematic studies in the literature from which to draw, or large variations in the solution composition are expected that will invalidate traditional methods (i.e., the specific ion interaction theory). In these cases, the observed molar absorptivity coefficients that are measured cannot be attributed to any given species but instead must be attributed to the combined effects of all species present in the solution. Therefore, the focus of these studies shifts from knowledge of the species present to knowledge of the solution chemistry (e.g., ligand or complexant concentration). The response curve of the metal analyte with respect to the solution chemistry will then be measured. In this way, concentration-dependent features, such as spectroscopically distinct dimers, will be included in the observed spectrum. These species will most likely present as deviations from a linear Beer's Law relationship.

The methodology detailed in this report has been developed to measure the molar absorptivity coefficients for transition, lanthanide and actinide metals where the speciation is unknown or is not readily available. This method will specifically focus on the effect of acid concentration (as a complexant) on the absorbance of metal ions. The limits are concentration of metal ions up to the gram per liter level, and acid concentrations above 0.1 molar and up to

commonly available concentrated acid. Concentrations will be specified in molarity and no consideration will be given to controlling ionic strength.

B.2 MATERIALS AND METHODS

The materials used in this method would be found in most analytical or quantitative analysis laboratories. Generally, no special lab ware, other than cuvettes, is required for sample handling and production. These materials include the following:

Spectrometer —A double-beam UV-vis spectrometer suitable for thermodynamic chemistry measurements should be used for these experiments. A Cary 100, Cary 5000, or similar spectrometer would be sufficient. The system should pass standard photometric accuracy, baseline flatness, and noise diagnostic tests as specified by the manufacturer. A wavelength range of at least 300–800 nm is preferable, but the wavelength range should be chosen to match the potential metals of interest. For example, hexavalent plutonium requires a spectrometer with a wavelength range up to 850 nm. Example spectrometers from the Cary line (www.chem.agilent.com) are shown in Figure B-1.

Cary 5000 UV-Vis-NIR Cary 100 UV-Vis

Figure B-1—Double-beam spectrometers from the Agilent Cary line. (© Agilent Technologies, Inc. 2015. Reproduced with Permission, Courtesy of Agilent Technologies, Inc.)

Cuvettes—Quartz cuvettes will be used throughout this methodology when feasible. Optionally, cuvettes may have a fluoropolymer or similar cap to reduce losses of valuable/hazardous materials. All cuvettes must have a certificate of compliance that states the path length and uncertainty of the cuvettes. Matched cuvettes must be used in the reference position for all cuvette types. If large numbers of samples will be generated, disposable cuvettes can be used (e.g., poly(methyl methacrylate) or PMMA) if the path length and path length uncertainty are provided or measured. Examples of available cuvettes, from Hellma Analytics (www.hellma-analytics.com), are shown in Figure B-2.

Figure B-2—Example macro, semi-micro, and micro volume cuvettes. (Photos provided courtesy of Hellma Analytics.)

Glassware—A suitable selection of Class A volumetric glassware will be available. Additional glass storage bottles and glassware (beakers, stirring rods, watch glasses, etc.) should also be available. All glassware should be leached in dilute (~0.1 M) nitric acid and rinsed in polished water[1] prior to use.

Analytical Balance—A balance with milligram or better resolution should be available for sample preparation. The balance should be calibrated as recommended by the manufacturer and should be periodically verified with suitable check masses.

Pipettes—A selection of pipettes must be available for use as needed. The pipette calibrations should be checked every day they are used. The calibration is checked by using the pipette to dispense a set volume of water, with a known temperature, onto a certified balance. This procedure is repeated a minimum of five times. Based on the known density of water and the mass, the mean water volume and standard deviation can be computed. This value should be compared to the pipette certification to ensure that the pipette is operating correctly.

Chemicals—All chemicals must be American Chemical Society grade reagents or higher grade where possible.[2] Certificates of analysis should be recorded for each chemical used.

[1] For the purposes of this method, polished water will be considered to be 18 MΩ·cm water obtained from a laboratory distribution system or high-purity water purchased from a reputable supplier.

[2] It is understood that actinide samples may not be available in a certified form.

B.3 STOCK AND SAMPLE PREPARATION

B.3.1 SAMPLE PLANNING

Because this method is applicable to high-value actinide and lanthanide elements, sample preparation will utilize single, high-concentration stock solutions to create all subsequent solutions for each metal analyte. This will minimize the number of high-value solutions created and subsequent waste generated. Care should be taken to create a metal stock solution with appropriate metal ion and acid concentrations such that the entire analytical range can be created from a single solution. Each stock solution should be made such that the ratio of the metal concentration (M_S) to the highest sample metal concentration planned (M_n) must be greater than or equal to the ratio of the stock acid concentration (A_S) to the lowest acid concentration planned (A_1). This will ensure that the proposed sample space can be generated from the stock solution.

> **Example**: If a 10-g/L copper solution in HCl stock solution is to be made and samples with a maximum of 2-g/L copper will be made from this, what concentration of acid will be required if the minimum acid level is 0.5 M? The metal ratio is 5, therefore the stock must contain no more than (5) × (0.5 M) = 2.5 M HCl. Acid concentrations any higher in the stock will prevent the creation of a 2-g/L, 0.5 M HCl sample.

> **Example**: A 100-g/L uranium solution in 12 M nitric acid exists. What is the highest metal ion concentration possible if the minimum acid concentration is 1 molar? The acid ratio is 12, therefore the maximum U level is (100 g/L)/(12) = 8.33 g/L. Any higher metal ion concentrations will have too much acid.

B.3.2 ACID SOLUTIONS

Acid solutions must be prepared for creation of samples via direct production or by dilution, either at a level that matches the acid concentration of the metal stock solution or at another appropriate calculated level. In addition, acid solutions will be prepared for all acid concentrations to be investigated. All acid solutions will be made by gravimetrically diluting concentrated acid with deionized water in acid-washed flasks. During the preparation of these samples, after approximately half of the required water has been added to the concentrated acid, the solution should be capped and allowed to cool prior to diluting to the mark. Aliquots of each solution should be taken for analysis.

B.3.3 METAL STOCK SOLUTIONS

To create the metal containing stock solutions, two methods may be employed. The methods for dry stock materials and dissolved stock materials are listed below.

B.3.3.1 Dry Samples

A known amount of the metal compound (salt, oxide, etc.) will be weighed out and quantitatively rinsed into a volumetric flask using the acid stock.[3] The metal stock solution is completed by diluting to the mark with the acid stock. Dilution with the acid stock will minimize the heat generated by the solution during mixing. Unless the compound is considered a primary standard, an aliquot will be taken for analysis to establish the metal ion concentration. Any acid consumed during the dissolution of the compound should be calculated and subtracted from the final acid concentrations. The final solution should give concentrations in molarity for both the acid and metal.

Alternately, if a gravimetric preparation is preferred, the metal will be weighed into an appropriate container and an appropriate amount of the desired acid stock solution will be added. As above, any acid consumed in the dissolution should be calculated and subtracted from the final total and an aliquot should be taken for analysis. The final solution concentrations should be expressed as grams of metal or acid per gram of solution.

B.3.3.2 Previously Dissolved Samples

If a metal solution with verified metal and acid concentrations exists, and can generate the desired samples for the experiment, proceed to the next section. For concentrated metal ion solutions without a known acid concentration or dilute solutions, assuming that an approximate mass of metal is known, the parent solution must be concentrated to the acid azeotrope to fix the acid concentration and maximize the metal concentration. This procedure should be performed using gentle heating in acid-washed Teflon lab ware. Care should be taken to avoid loss of material during the concentration procedure (e.g., due to spattering). If the metal ion concentration is expected to surpass the solubility limit, dilute the sample with small volumes of concentrated acid until all of the metal has been solubilized.

Once the acid concentration is established, the solution will be transferred to a weighed vial. Based on the approximately known metal mass, the grams of metal (or metal salt) and acid per gram of solution can be estimated. If the stock solution needs to be diluted, it will be gravimetrically diluted with dilute acid solution until the desired acid concentration is reached. Heat will be generated by the dilution of the concentrated acid, and the solution should be sealed and allowed to cool prior to proceeding. Finally, the metal stock solution will be finished by dilution with a matching acid stock solution. An aliquot of this solution should be taken for analysis. Once the total amount of metal is determined, the final metal and acid concentrations (in gram analyte per gram solution) can be fixed.

[3] For hygroscopic salts, the salts should be stored under dry, inert gas in a desiccator.

B.3.4 SOLUTION DENSITIES

The density of all solutions, regardless of preparation, should be measured. Using a calibrated pipette, known volumes of solutions are weighed and the solution densities are calculated. Alternately, if there is enough solution, the solution density can be measured by adding the solution to a pre-weighed 5- or 10-mL volumetric flask. The filled flask is then weighed and the solution density is computed. The volumetric flask provides a certified volume, with uncertainty, for the error propagation.

B.3.5 SAMPLE PREPARATION

Once metal and acid stocks have been made, two methods may be employed to generate individual analytical samples. In the first method (direct production), individual samples will be produced directly with fine control over metal and acid concentrations. The second method (dilution) creates parent solutions that are systematically diluted to create a series of samples with varying metal concentrations at a fixed acid concentration. Each methodology has advantages. The direct production method creates very well-defined samples and can be easily tailored to make specific samples. It does require more starting material and produces more waste, which can be a drawback. The dilution method can generate many samples from a small initial amount of metal stock, although the metal ion concentration decreases in a non-linear fashion over the course of the experiment and specific metal ion concentrations cannot be achieved.

B.3.5.1 Direct Production

By directly producing each sample from appropriate stock solutions, a very specific set of samples can be made. All additions can be made volumetrically if class A glassware and calibrated pipettes are used or gravimetrically if the solution densities are known (or have been measured).[4] In order to produce samples with consistent acid concentrations, but varying metal ion concentrations, three additions will be made. An aliquot of the metal stock solution will be added followed by an aliquot of the matching acid stock solution. The total volume (mass) of these two additions will remain constant to fix the amount of acid being added. These solutions are then diluted to their final volumes (masses) with the appropriate sample acid stock solution.

> **Example**: A 10-g/L Cr^{3+}, 10 M HCl stock solution is prepared along with 1, 3, 5.5, 8, and 10 molar HCl solutions. Samples with metal concentrations of 0.1, 0.5, and 1.0 g/L are to be investigated, each with a total volume of 10 mL. The first sample is created from 0.1 mL metal stock followed by 0.9 mL 10 M HCl, the next from 0.5 mL metal stock and 0.5 mL 10 M HCl, and the third from 1 mL metal stock. Each sample is then diluted to 10 mL using 1 M acid using volumetric flasks. In this case, each solution has a final

[4] For the purposes of this method, stock solutions with metal ion concentrations up to several g/L and acid concentrations of at least 1 mol/L are assumed to not appreciably change the solution density from that of the acid. However, the experimenter is encouraged to measure solution densities whenever possible.

acidity of 2.35 molar. This method would then be repeated with the other acid stocks, resulting in sample sets with acidities of 4.05, 6.18, 8.30, and 10 molar, respectively.

Example: A stock solution with 1 g/L Fe in 6 M HCl is prepared along with 1–6 M acid solutions. Metal concentrations at approximately 1.0, 2.5, and 4.0% of the stock concentration are to be made. The first sample is created from 0.10 g of the stock solution, 0.90 g of the 6 M acid. The second from 0.25 g and 0.75 g of the metal and acid solutions, respectively, and the third from 0.40 g and 0.60 g. Each of these solutions is diluted to 10 g using the 1 M acid.

Due to contributions from the two stock solutions, the final sample will have an acid concentration slightly higher than the prepared sample acid solution. This methodology is useful for preparing samples within a pre-defined set of conditions, particularly if regularly spaced or non-inclusive sample sets are required. It is assumed that the metal stock solution and the corresponding acid solution have negligibly different densities. If known, the metal solution density should be used throughout these calculations when required.

B.3.5.2 Dilution

When using high-value metals, it may be impractical to make several stock solutions and create large volume samples directly. In these situations, sequential dilution of a parent solution with an acid standard will provide a series of samples at a constant acid concentration and exponentially decreasing concentration. This allows a single aliquot of metal to generate samples that cover 2–3 orders of magnitude in concentration with a reasonable number of samples (10–15). Due to the nature of the dilution, this method must be carried out gravimetrically.

To do this, parent solutions are made using the direct production method above with metal concentrations at the top of the desired range and acid concentrations at the desired levels. Each acid concentration should have a matching acid stock solution for dilutions (see above). A known mass of each parent solution is placed in a Teflon beaker with a Teflon-coated magnetic stir bar and placed on a stir plate. An aliquot of the solution is taken from the parent solution and placed in a cuvette. This aliquot is taken using a calibrated pipette and the volume is noted. New masses are taken for the parent solution and the cuvette. An aliquot of the acid diluent is then added to the parent solution and the solution is re-weighed. The procedure is repeated as necessary. The specific masses of the parent solution and the aliquots are adjustable parameters left to be determined on a case-by-case basis.

Example: A 10 mM solution of uranium is prepared with a nitric acid concentration of 7 mol/L. A 1.75-mL aliquot of this solution is placed in a Teflon beaker. The metal solution has a density of 1.22 g/L. The total mass of the solution is 2.135 g. A 0.7-mL aliquot is placed in a cuvette. The mass of the beaker is recorded as 1.281 g. A 0.7-mL aliquot is added to the beaker, the solution is allowed to stir and the mass is recorded again to be 2.135 g. The new metal concentration is 6 mM. The process is then repeated to create samples with metal concentrations of 3.6 mM, 2.16 mM, and so on. The process is repeated until the desired range of metal concentrations has been produced.

The example above ignores any mass losses due to pipette residues or errors. This method also requires sequential calculations to determine the exact concentration of each sample. Aliquots of several samples should be taken for independent concentration measurements and to ensure that the dilution was performed correctly.

B.4 DATA COLLECTION

All samples will be placed in cuvettes and cleaned with a lint-free cloth prior to analysis. The reference position of the spectrometer should be filled with a water-filled cuvette The spectrometer should be zeroed with water-filled cuvettes in both positions. A baseline spectrum should then be collected and subtracted from all subsequent samples.

The specific data collection parameters will vary depending on the spectrometer used. The following recommendations are provided as general guidance.

- The data interval should be no greater than 1 nm.
- The data averaging time should be no less than 0.1 s (equivalent to a scan rate of 600 nm/min).
- The slit width should be reduced as much as reasonably possible to increase peak resolution/sharpness.
- The beam height should be adjustable to fall in the center of the solution (if adjustable).

B.5 CALCULATION OF SOLUTION PROPERTIES AND PROPAGATION OF ERROR

In this section, the various calculations that are required will be laid out. To keep the various parameters clear, a listing of all different variables is presented here.

- m_X—mass of a solution or dry compound X
- ρ_X—density of solution X
- V_X—volume of solution X
- A_S—acid stock solution
- M_S—metal stock solution
- A_n—n^{th} acid solution
- M_n—n^{th} metal solution
- RM_n—reduced volume metal solution (dilution method)
- S_n—aliquot removed from solution M_n to create RM_n during the dilution method
- $C_{A(X)}$—acid concentration of solution X
- $C_{M(X)}$—metal concentration of solution X
- R—stoichiometric ratio between two species in a balanced chemical reaction

B.5.1 MASS MEASUREMENTS

For all mass measurements in this work, a common feature is the use and inflation of mass errors. This is due to the relative nature of most mass measurements where the difference in two masses is computed as opposed to the absolute mass of an item. For example, a measurement of a liquid is performed by measuring the mass of a beaker before and after the aliquot is added and the difference is computed. This computation of net masses results in a small inflation in the error of the measurements, as stated below. In these cases (assuming the same balance was used), the error in each measurement will be identical and the equation will reduce. If two different balances were used (not recommended) then the simplification cannot be used. In this method, it is assumed that the same balance is made for both measurements and pursuantly the inflation has been included in all calculations as appropriate.

Note on differential masses (EO):

$$m_{net} = m_{gross} - m_{tare} \qquad \partial m_{net} = \left(\left(\partial m_{Gross}\right)^2 + \left(\partial m_{tare}\right)^2\right)^{1/2} = \left(2\partial m^2\right)^{1/2} = \sqrt{2}\partial m$$

$$\frac{\partial m_{net}}{m_{net}} = \frac{\sqrt{2}\partial m}{m_{net}}$$

B.5.2 ACID SOLUTIONS

Aliquots of each acid stock solution will be taken and archived for analysis. The nominal acidity of each solution will be calculated based on the gravimetric dilution and acid certificate of analysis. Each solution (A_n) will be prepared gravimetrically. The stock molarity ($C_{A(As)}$), the solution masses (m_{As}, m_{An}), and the balance error (δm) are required. The solution densities and errors (ρ_{As}, ρ_{An}, $\delta\rho_{As}$, and $\delta\rho_{An}$) should be known or measured. A propagated error will then be calculated and reported with the nominal concentration.

Standard Solution Molarity (E1):

$$C_{A(An)} = \frac{C_{A(As)} m_{As} \rho_{An}}{m_{An} \rho_{As}} \qquad \frac{\partial C_{A(An)}}{C_{A(An)}} = \left(\left(\frac{\partial C_{A(As)}}{C_{A(As)}}\right)^2 + \left(\frac{\sqrt{2}\partial m}{m_{As}}\right)^2 + \left(\frac{\sqrt{2}\partial m}{m_{An}}\right)^2 + \left(\frac{\partial \rho_{As}}{\rho_{As}}\right)^2 + \left(\frac{\partial \rho_{An}}{\rho_{An}}\right)^2\right)^{1/2}$$

B.5.3 DENSITIES

In order to calculate the solution densities, the mass and volume of each solution is recorded by dispensing aliquots into pre-weighed vials. A pipette with a verified calibration must be used. Alternately, a volumetric flask can be used instead of a vial and pipette.

Density (E4):

$$\rho_X = \frac{m_X}{V_X} \qquad \frac{\partial \rho_X}{\rho_X} = \left(\left(\frac{\sqrt{2}\partial m}{m_X}\right)^2 + \left(\frac{\partial V_X}{V_X}\right)^2\right)^{1/2}$$

B.5.4 METAL SOLUTIONS

Aliquots of the metal stock solution (M_s) will be sent for analysis by inductively coupled plasma mass spectrometry (ICP-MS) or atomic emission spectrometry (ICP-AES) or a similar technique. These analyses will provide both the stock solution metal concentration ($C_{M(Ms)}$) and its associated error ($\delta C_{M(Ms)}$). The concentration should be reported in both concentration (mol/L) and weight percent (g/g solution). In addition to the metal concentration, the acid concentration of the stock must be determined.

For solutions made from metal salts, the acid concentration ($C_{A(Ms)}$) will be the same as the diluent used. If the metal existed in a form that will not dissolve directly and must be oxidized or reduced (i.e., a metal or a high oxide) the amount of acid consumed must be calculated and subtracted from the total acid present ($C'_{A(Ms)}$). Based on the balanced reaction equation, a stoichiometric ratio (R) of acid consumed must be calculated.

Metal acid concentration—dry materials (E2):

$$C_{A(Ms)} = C'_{A(Ms)} - (R)(C_{M(Ms)}) \qquad \partial C_{A(Ms)} = \left(\left(\partial C'_{A(Ms)}\right)^2 + \left(\partial C_{M(Ms)}\right)^2\right)^{1/2}$$

Metal stocks derived from previously dissolved materials pose a more difficult challenge. In these situations, the acid concentration in the source solution is assumed to be present at its azeotrope. An aliquot of this material with a known volume will then be diluted to make a suitable stock solution (following E5–E7 below). By measuring the concentration of the final metal stock in weight percent ($C_{M(Mn)}$) and correcting for dilution, the mass of concentrated acid added can be calculated. The form of the metal must be taken into account as the mass of the metal must be converted to represent the metal salt.

Metal acid concentration—dissolved materials (E3):

$$C_{M(Ms)} = \frac{C_{M(Mn)} V_{Mn}}{V_{Ms}} \qquad \frac{\partial C_{M(Mn)}}{C_{M(Mn)}} = \left(\left(\frac{\partial C_{M(Ms)}}{C_{M(Ms)}}\right)^2 + \left(\frac{\partial V_{Ms}}{V_{Ms}}\right)^2 + \left(\frac{\partial V_{Mn}}{V_{Mn}}\right)^2\right)^{1/2}$$

$$C_{A(Ms)} = 1 - \left(\frac{C_{M(Ms)} \cdot MW_{Salt}}{MW_{Metal}}\right) \qquad \frac{\partial C_{A(Ms)}}{C_{A(Ms)}} = \frac{\partial C_{A(Ms)}}{C_{A(Ms)}}$$

B.5.5 SAMPLES

Each individual sample will need to have the uncertainty of the metal and acid concentrations propagated throughout each experiment. These uncertainties will be used in the determination of the molar absorptivity constants.

B.5.5.1 Direct Production

For each of these samples, the metal and acid concentration errors follow the standard error propagation rules. The total contribution of either quantity is calculated, along with the error, followed by the total volume and error. Finally, the two are combined for the concentration measurements. For all gravimetrically prepared solutions, the total solution mass and density (calculated above) will be used to determine the solution volume. If a volumetric flask is used, the total error on the volume will be according to the error on the flask. The amount of metal ion present is calculated by using a known volume or a known mass/density and using the standard dilution formula.

Total volume (E5):

$$V_{Mn} = \frac{m_{Mn}}{\rho_{Mn}} \qquad \frac{\partial V_{Mn}}{V_{Mn}} = \left(\left(\frac{\sqrt{2}\partial m}{m_{Mn}} \right)^2 + \left(\frac{\partial \rho_{Mn}}{\rho_{Mn}} \right)^2 \right)^{1/2}$$

Metal concentration (E6):

$$C_{M(Mn)} = \frac{C_{M(Ms)} V_{Ms}}{V_{Mn}} \; or \; \frac{C_{M(Ms)} m_{Ms}}{V_{Mn} \rho_{Ms}} \qquad \frac{\partial C_{M(Mn)}}{C_{M(Mn)}} = \left(\left(\frac{\partial C_{M(Ms)}}{C_{M(Ms)}} \right)^2 + \left(\frac{\partial V_{Ms}}{V_{Ms}} \right)^2 + \left(\frac{\partial V_{Mn}}{V_{Mn}} \right)^2 \right)^{1/2}$$

$$\text{where } \frac{\partial V_x}{V_x} = \left(\left(\frac{\sqrt{2}\partial m}{m_x} \right)^2 + \left(\frac{\partial \rho_x}{\rho_x} \right)^2 \right)^{1/2}$$

To calculate the acid concentration of the samples, the total number of moles of acid must be determined. Unlike the metal calculation, each solution added to the sample has some amount of acid present. Each individual contribution is found by multiplying the concentration ($C_{A(X)}$) by the volume (V_X), or by the gram mass (m_X) and dividing by the density (ρ_X) as in E5, and summing to determine the total moles. This is then divided by the total volume. When using a volumetric flask, the last acid addition is not explicitly measured as the flask is filled to the mark. Therefore, the volume of acid added must be estimated. It is understood that this particular operation adds a small amount of error but will have a negligible effect on the total error in the acid concentration.

Acid concentration (E7):

$$C_{A(Mn)} = \frac{C_{A(Ms)}V_{Ms} + C_{A(As)}V_{As} + C_{A(An)}V_{An}}{V_{Mn}} = \frac{C_{A(Ms)}V_{Ms}}{V_{Mn}} + \frac{C_{A(As)}V_{As}}{V_{Mn}} + \frac{C_{A(An)}V_{An}}{V_{Mn}}$$

where $V_{An} = V_{Flask} - (V_{Ms} + V_{As})$

$$\partial C_{A(Mn)} = \left(\begin{array}{l} \left(\left(\frac{\partial C_{A(Ms)}}{C_{A(Ms)}} \right)^2 + \left(\frac{\partial V_{Ms}}{V_{Ms}} \right)^2 + \left(\frac{\partial V_{Mn}}{V_{Mn}} \right)^2 \right) \left(\frac{C_{A(Ms)}V_{Ms}}{V_{Mn}} \right)^2 + \ldots \\ \ldots + \left(\left(\frac{\partial C_{A(As)}}{C_{A(As)}} \right)^2 + \left(\frac{\partial V_{As}}{V_{As}} \right)^2 + \left(\frac{\partial V_{Mn}}{V_{Mn}} \right)^2 \right) \left(\frac{C_{A(As)}V_{As}}{V_{Mn}} \right)^2 + \ldots \\ \ldots + \left(\left(\frac{\partial C_{A(An)}}{C_{A(An)}} \right)^2 + \left(\frac{\partial V_{An}}{V_{An}} \right)^2 + \left(\frac{\partial V_{Mn}}{V_{Mn}} \right)^2 \right) \left(\frac{C_{A(An)}V_{An}}{V_{Mn}} \right)^2 \end{array} \right)^{1/2}$$

where $\partial V_{An} = \left(\partial V_{Flask}{}^2 + \partial V_{Ms}{}^2 + \partial V_{As}{}^2 \right)^{1/2}$

B.5.6 DILUTION

Determination of the metal and acid concentrations and their uncertainties must be done stepwise throughout the dilution. For every sample, the new metal and acid concentrations are calculated by calculating the dilution factor and propagating the error. This is done by recording masses throughout the dilution. The use of a calibrated pipette is also required to determine the solution density at each step. During the experiment, three quantities are recorded for each sample, P_n: the starting solution mass, m_{Pn}; the volume of the sample aliquot taken, V_{Sn}; and the reduced solution mass, m_{PRn}. After addition of the diluent acid (A_n), the next sample, P_{n+1}, is created. The recorded mass of P_{n+1} is then used to start the next set of data calculations (i.e., m_{P+1}).

For all calculations, net masses must be used. First the density of each solution must be calculated. The density is determined from the three values recorded at each value of n. This is followed by the calculation of the metal concentration and the acid concentration. Due to the iterative and calculation intense nature of this process, a spreadsheet utility is recommended.

Density (E8):

$$\rho_{Mn} = \frac{m_{Mn} - m_{RMn}}{V_{Sn}} \qquad \frac{\partial \rho_{Mn}}{\rho_{Mn}} = \left(\left(\frac{2\partial m}{m_{Mn} - m_{RMn}} \right)^2 + \left(\frac{\partial V_{Sn}}{V_{Sn}} \right)^2 \right)^{1/2}$$

Metal Concentration (E9):

$$C_{M(Mn)} = C_{M(Mn-1)} \frac{m_{RMn-1}\rho_{Mn}}{\rho_{Mn-1}m_{Mn}}$$

$$\frac{\partial C_{M(Mn)}}{C_{M(Mn)}} = \left(\left(\frac{\partial C_{M(Mn-1)}}{C_{M(Mn-1)}} \right)^2 + \left(\frac{\sqrt{2}\partial m}{m_{RMn-1}} \right)^2 + \left(\frac{\partial \rho_{Mn}}{\rho_{Mn}} \right)^2 + \left(\frac{\partial \rho_{Mn-1}}{\rho_{Mn-1}} \right)^2 + \left(\frac{\sqrt{2}\partial m}{m_{Mn}} \right)^2 \right)^{1/2}$$

Acid Concentration (E10):

$$C_{A(Mn)} = \frac{\left(\frac{m_{RMn-1}}{\rho_{Mn-1}} \right) C_{A(Mn-1)} + \left(\frac{m_{Mn} - m_{RMn-1}}{\rho_{An}} \right) C_{A(An)}}{\left(\frac{m_{Mn}}{\rho_{Mn}} \right)} = \frac{m_{RMn-1}\rho_{Mn}C_{A(Mn-1)}}{m_{Mn}\rho_{Mn-1}} + \frac{(m_{Mn} - m_{RMn-1})\rho_{Mn}C_{A(An)}}{m_{Mn}\rho_{An}}$$

$$\partial C_{A(Mn)} =$$

$$\left(\left(\left(\frac{\sqrt{2}\partial m}{m_{RMn-1}} \right)^2 + \left(\frac{\partial \rho_{Mn}}{\rho_{Mn}} \right)^2 + \left(\frac{\partial C_{A(Mn-1)}}{C_{A(Mn-1)}} \right)^2 + \left(\frac{\sqrt{2}\partial m}{m_{Mn}} \right)^2 + \left(\frac{\partial \rho_{RMn-1}}{\rho_{Mn-1}} \right)^2 \right) \left(\frac{m_{RMn-1}\rho_{Mn}C_{A(Mn-1)}}{m_{Mn}\rho_{Mn-1}} \right)^2 + \ldots \right.$$
$$\left. \ldots \left(\left(\frac{2\partial m}{m_{Mn} - m_{RMn-1}} \right)^2 + \left(\frac{\partial \rho_{Mn}}{\rho_{Mn}} \right)^2 + \left(\frac{\partial C_{A(An)}}{C_{A(An)}} \right)^2 + \left(\frac{\sqrt{2}\partial m}{m_{Mn}} \right)^2 + \left(\frac{\partial \rho_{An}}{\rho_{An}} \right)^2 \right) \left(\frac{(m_{Mn} - m_{RMn-1})\rho_{Mn}C_{A(An)}}{m_{Mn}\rho_{An}} \right)^2 \right)^{1/2}$$

B.6 CALCULATION OF MOLAR ABSORPTIVITY COEFFICIENTS

In order to adequately determine the molar absorptivity coefficient of any element, it is not sufficient to simply measure the concentration of the element and its absorption. This single point method will not reveal any behavior that deviates from Beer's law. Therefore, a series of metal ion concentrations under the same solution conditions will need to be measured. Not only will this determine the shape of the response curve (linear vs. curvilinear), it will determine the molar absorptivity via a curve regression.

A standard approach to determine the molar absorptivity coefficient of a metal species is to produce a set of metal ion solutions and measure the absorbance of selected peaks in each sample. Inherent in this method is the assumption that the metal ion solution concentration is known *exactly* with little-to-no uncertainty. However, unless the metal of interest is a primary standard, this assumption will not hold. Therefore, there will be an uncertainty associated with the metal ion concentration, and a propagated uncertainty for all dilutions of that solution. Because all solutions in this method are dilutions of a stock solution, each solution will have a propagated uncertainty associated with it.

If one assumes that there is an uncertainty in the absorbance measurement and in the pathlength of the cuvette used, then the data regression and interpretation becomes very convoluted; there is an uncertainty in both variables and in one of the constant terms. This is indeed the case because, despite improvements in spectroscopic hardware, repeated

spectroscopic measurements will have a small, but significant, error. In addition, there is a non-negligible error in the pathlength of the cuvettes used to make the measurements. Propagation of these errors throughout the data analysis is accomplished by a numerical estimation routine (see below). Both the MATLAB® and Scilab scripts are included in this appendix.

The numerical program, titled ALE (Absorptivity Linear Estimator) uses a maximum likelihood estimator routine to produce the best fit to the experimental data and produce a molar absorptivity coefficient with a model error. This method is novel insofar as it provides a rigorous method for estimating the error of the molar absorptivity coefficient of a species at a given wavelength.

B.6.1 MATLAB®

A MATLAB® script was written to estimate the molar absorptivity coefficient (ε), and the uncertainty in the coefficient, given absorbance values (*a*), concentrations (*c*), and pathlength values (*l*). Although this application of Beer's law may seem trivial, the mechanics of estimating the molar absorptivity coefficient and propagating its uncertainty when there is uncertainty in all three input terms is far from simple. To solve this problem, a numerical method using a maximum likelihood estimation was developed (by the MCS division of Argonne). This method assumes (1) that the noise in the various quantities are independent and (2) that the values of the individual quantities (*a*, *c*, and *l*) are large enough that the probability that the true mean of any of these points is negative is negligible.

Briefly, the estimation of ε is performed by optimizing the objective function (shown below). The first and second derivatives of this equation are calculated and function minima are considered to be solutions to the equation. The standard error is defined as the inverse square root of the Hessian of the objective function:

$$\max_{\varepsilon} \prod_{i=1}^{n} \left(\frac{1}{\sqrt{2\pi\left(\left(\varepsilon l \sigma_{c_i}\right)^2 + (\epsilon \sigma_i \sigma_l)^2 + \sigma_{a_i}^2\right)}} e^{-\frac{(a_i - \varepsilon c_i l)^2}{2\left(\left(\varepsilon l \sigma_{c_i}\right)^2 + (\epsilon \sigma_i \sigma_l)^2 + \sigma_{a_i}^2\right)}} \right)$$

B.6.2 INPUT FILES

The MATLAB® code for ALE requires six inputs in order to produce an estimate of the molar absorptivity coefficient: sample absorbance values, the concentration values, the path length value, and the propagated or measured uncertainty values for these values. These files are formatted tab delimited files. The tolerance (TOL) of the routine must be specified. This level determines the maximum size of the variation in the refined values between iterations. Once successive iterations vary by less than the tolerance, the program will be considered to have converged. By default, the tolerance is set to 1×10^{-8} (1E-8). Finally, an initial estimate of the molar absorptivity is also required.

Example of formatted data for the MATLAB® program. Each column would be separated into a separate *dat* file without the header information.

Concentration	Absorbance	Pathlength
8.08E-02	7.89E-01	1
5.94E-02	5.74E-01	
4.04E-02	4.10E-01	
1.90E-02	1.80E-01	
1.05E-02	1.25E-01	
8.08E-03	9.93E-02	
5.94E-03	6.46E-02	
4.04E-03	4.64E-02	
1.90E-03	2.25E-02	
9.50E-04	9.22E-03	

B.6.2.1 Code

```
%{
The data files A.dat, C.dat are tab delimited text documents that contain the absorbance and
concentration values for all samples. The L.dat file contains the pathlength of the cuvettes used.
The uncertainties in this program are calculated based on fixed uncertainties. If individual
uncertainties are known, they can be loaded as separate dat files in the place of the calculations.
The input files should be located in the same directory as the program. The value of each
uncertainty must be manually entered for each run.
%}

load a.dat;
load c.dat;
load l.dat;

sigma_a = 0.001*ones(length(a),1);
sigma_c = 0.05*c;
sigma_l = 0.005*l;

tol = 1e-8;
e = 100000;

while (1)
 f = 0.5 * ones(1, length(a)) * (log((e*c*sigma_l).^2 + (e*sigma_c*l).^2 + sigma_a.^2) + (a -
e*c*l).^2 ./ ((e*c*sigma_l).^2 + (e*sigma_c*l).^2 + sigma_a.^2) + log(2*pi));

 df = ones(1, length(a)) * ((e*(c*sigma_l).^2 + e*(sigma_c*l).^2) ./ ((e*c*sigma_l).^2 +
(e*sigma_c*l).^2 + sigma_a.^2) + (e*(c*l).^2 - a.*c*l) ./ ((e*c*sigma_l).^2 + (e*sigma_c*l).^2 +
sigma_a.^2) - (a - e*c*l).^2 .* (e*(c*sigma_l).^2 + e*(sigma_c*l).^2) ./ ((e*c*sigma_l).^2 +
(e*sigma_c*l).^2 + sigma_a.^2).^2);
```

```
 hf = ones(1, length(a)) * (((c*sigma_l).^2 + (sigma_c*l).^2) ./ ((e*c*sigma_l).^2 +
(e*sigma_c*l).^2 + sigma_a.^2) - 2*(e*(c*sigma_l).^2 + e*(sigma_c*l).^2).^2 ./
((e*c*sigma_l).^2 + (e*sigma_c*l).^2 + sigma_a.^2).^2 + (c*l).^2 ./ ((e*c*sigma_l).^2 +
(e*sigma_c*l).^2 + sigma_a.^2) - 2*(e*(c*l).^2 - a.*c*l).*(e*(c*sigma_l).^2 + e*(sigma_c*l).^2) ./
((e*c*sigma_l).^2 + (e*sigma_c*l).^2 + sigma_a.^2).^2 - 2*(e*c*l-a).*c*l .* (e*(c*sigma_l).^2 +
e*(sigma_c*l).^2) ./ ((e*c*sigma_l).^2 + (e*sigma_c*l).^2 + sigma_a.^2).^2 - (e*c*l-a).^2 .*
((c*sigma_l).^2 + (sigma_c*l).^2) ./ ((e*c*sigma_l).^2 + (e*sigma_c*l).^2 + sigma_a.^2).^2 +
4*(e*c*l-a).^2 .* (e*(c*sigma_l).^2 + e*(sigma_c*l).^2).^2 ./ ((e*c*sigma_l).^2 +
(e*sigma_c*l).^2 + sigma_a.^2).^3);

 e, f, df, hf
 if (abs(df) < tol)
  break;
 endif

 e = e - df / hf;
end

e
sigma = sqrt(1/hf)
```

B.6.3 SCILAB

The MATLAB® program above was converted to the open source Scilab code. This code requires seven formatted input files. Once the program is loaded, the code needs to be modified to specify the local directory of the input files. The tolerance of the routine must be specified. This level determines the maximum size of the variation in the refined values between iterations. Once successive iterations vary by less than the tolerance, the program will be considered to have converged. By default, the tolerance is set to 1E-8.

B.6.3.1 Input Files

The input files for the Scilab code are seven tab delimited text files of the sample absorbance values, the uncertainty in the absorbance values, the sample concentrations, the concentration uncertainties, the pathlength of the cuvettes used, the error of the cuvette path length, and an initial estimate of the molar absorptivity coefficient.

Example: Formatted data for the Scilab program. Each column would be separated into a separate txt file without the header information.

Concentration	Concentration Uncertainty	Absorbance	Absorbance Uncertainty	Pathlength	Pathlength Uncertainty	Initial Molar Absorptivity Estimate
8.08E-02	4.00E-03	7.89E-01	1.84E-04	1	0.005	10
5.94E-02	3.00E-03	5.74E-01	2.02E-04			
4.04E-02	2.00E-03	4.10E-01	3.93E-04			
1.90E-02	1.00E-03	1.80E-01	1.14E-04			
1.05E-02	5.00E-04	1.25E-01	3.21E-04			
8.08E-03	4.00E-04	9.93E-02	4.08E-04			
5.94E-03	3.00E-04	6.46E-02	6.32E-05			
4.04E-03	2.00E-04	4.64E-02	1.73E-04			
1.90E-03	1.00E-04	2.25E-02	1.77E-04			
9.50E-04	5.00E-05	9.22E-03	1.23E-04			

B.6.3.2 Code

```
//ABSORPTIVITY LINEAR ESTIMATOR VERSION 1.0 2014-02-04
//Users must replace \\LOCAL_PATH\ with the appropriate file directory where the input files
are
//stored, e.g. C:\Program Files\ALE\
a=fscanfMat("\\LOCAL_PATH\absorbance.txt")
c=fscanfMat("\\LOCAL_PATH\concentration.txt")
l=fscanfMat("\\LOCAL_PATH\pathlength.txt")
sigma_a=fscanfMat("\\LOCAL_PATH\Sigma_abs.txt")
sigma_c=fscanfMat("\\LOCAL_PATH\Sigma_conc.txt")
sigma_l = fscanfMat("\\LOCAL_PATH\Sigma_path.txt")
tol=1e-8
e=fscanfMat("\\LOCAL_PATH\e_est.txt")

while(1)
  f = 0.5 * ones(1, length(a)) * (log((e*c*sigma_l).^2 + (e*sigma_c*l).^2 + sigma_a.^2) + (a -
e*c*l).^2 ./ ((e*c*sigma_l).^2 + (e*sigma_c*l).^2 + sigma_a.^2) + log(2*%pi))

  df=ones(1, length(a)) * ((e*(c*sigma_l).^2 + e*(sigma_c*l).^2) ./ ((e*c*sigma_l).^2 +
(e*sigma_c*l).^2 + sigma_a.^2) + (e*(c*l).^2 - a.*c*l) ./ ((e*c*sigma_l).^2 + (e*sigma_c*l).^2 +
sigma_a.^2) - (a - e*c*l).^2 .* (e*(c*sigma_l).^2 + e*(sigma_c*l).^2) ./ ((e*c*sigma_l).^2 +
(e*sigma_c*l).^2 + sigma_a.^2).^2)

  hf=ones(1, length(a)) * (((c*sigma_l).^2 + (sigma_c*l).^2) ./ ((e*c*sigma_l).^2 +
(e*sigma_c*l).^2 + sigma_a.^2) - 2*(e*(c*sigma_l).^2 + e*(sigma_c*l).^2).^2 ./
((e*c*sigma_l).^2 + (e*sigma_c*l).^2 + sigma_a.^2).^2 + (c*l).^2 ./ ((e*c*sigma_l).^2 +
(e*sigma_c*l).^2 + sigma_a.^2) - 2*(e*(c*l).^2 - a.*c*l).*(e*(c*sigma_l).^2 + e*(sigma_c*l).^2) ./
((e*c*sigma_l).^2 + (e*sigma_c*l).^2 + sigma_a.^2).^2 - 2*(e*c*l-a).*c*l .* (e*(c*sigma_l).^2 +
```

```
e*(sigma_c*l).^2) ./ ((e*c*sigma_l).^2 + (e*sigma_c*l).^2 + sigma_a.^2).^2 - (e*c*l-a).^2 .*
((c*sigma_l).^2 + (sigma_c*l).^2) ./ ((e*c*sigma_l).^2 + (e*sigma_c*l).^2 + sigma_a.^2).^2 +
4*(e*c*l-a).^2 .* (e*(c*sigma_l).^2 + e*(sigma_c*l).^2).^2 ./ ((e*c*sigma_l).^2 +
(e*sigma_c*l).^2 + sigma_a.^2).^3)

  e,f,df,hf

  if abs(df)<tol then

    break

  end

  e = e-df/hf

  sigma_e=sqrt(1/hf)

  disp(e,"Molar Absorptivity: ")

  disp(sigma_e,"Model Error: ")

end
```

Nuclear Engineering Division
Argonne National Laboratory
9700 South Cass Avenue, Bldg. 205
Argonne, IL 60439-4854

www.anl.gov

Argonne National Laboratory is a U.S. Department of Energy
laboratory managed by UChicago Argonne, LLC